IMPROVED DROUGHT EARLY WARNING AND FORECASTING TO STRENGTHEN PREPAREDNESS AND ADAPTATION TO DROUGHTS IN AFRICA

DEWFORA

A 7th Framework Programme Collaborative Research Project

Integration of Drought Vulnerability and Hazards into Risk maps at the Pan-African level.

WP6-D6.4

February 2013

Coordinator:	Deltares, The Netherlands
Project website:	www.dewfora.net
FP7 Call	ENV-2010-1.3.3.1
Contract no.	265454

Page intentionally left blank

DOCUMENT INFORMATION

Title	**Integration of drought vulnerability and hazard into risk maps at the Pan-African level**
Lead Author	JRC
Contributors	UPM, DELTARES, ICPAC
Distribution	PP: Restricted to other programme participants (including the Commission Services)
Reference	WP6-D6.4

DOCUMENT HISTORY

Date	Revision	Prepared by	Organisation	Approved by	Notes
05/11/2012	0	Gustavo Naumann	JRC		
04/12/2012	1	Gustavo Naumann Ana Iglesias Luis Garrote Ruth Cuningham	JRC UPM		
14/12/2012	2	Gustavo Naumann Paulo Barbosa	JRC		
11/01/2013	3	Gustavo Naumann Paulo Barbosa	JRC		
24/01/2013	4	Gilbert Ouma	ICPAC		
18/02/2013	5	Gustavo Naumann Paulo Barbosa	JRC		

ACKNOWLEDGEMENT

The research leading to these results has received funding from the European Union's Seventh Framework Programme (FP7/2007-2013) under grant agreement N°265454

Page intentionally left blank

SUMMARY

Drought risk in this research was related to the capacity of a social system to cope, resist and recover (vulnerability) from any certain impact produced by a natural hazard. This hazard is an independent external factor that is defined by an overall frequency of occurrence of droughts with different intensity and duration.

A drought vulnerability index was constructed using socio-economic data at country level. This indicator is able to represent the complex processes that could lead to social drought vulnerability. However, it must be used critically taking into account that their construction relies on some level of subjectivity and theoretical assumptions. According to this analysis, the countries classified with higher relative vulnerability are Somalia, Mali, Ethiopia, Niger, Burundi and Chad.

A regional drought risk analysis shows that the basins with high to moderate drought risk can be subdivided in three main different geographical regions: the Mediterranean coast of Africa (comprising most of the Moroccan and Algerian basins and the Nile Delta); the Sub-Sahara and the south of Sahel regions (including the Volta, Niger, White and Blue Nile); the Serengeti and the Eastern Miombo woodlands of Tanzania and Mozambique. Additionally, the eastern part of the Zambezi basin, the South-eastern border of the Congo basin and the belt of Fynbos in the Western Cape should also be included in this category.

Even if the results are not conclusive, a good agreement is observed between the drought vulnerability and risk maps and the number of persons affected by droughts. There is a need to validate the vulnerability indicator with appropriate disaster data in order to measure and improve the robustness of the indicator and explain why in some cases extreme droughts can lead to disasters while in other cases their impact is much lower.

Page intentionally left blank

TABLE OF CONTENTS

LIST OF FIGURES

LIST OF TABLES

Page intentionally left blank

1. INTRODUCTION

The risk associated with drought for any specific region is a product of the region's exposure to the event (probability of drought occurrence at various severity levels) and the vulnerability of society to the event. Usually meteorological drought is a result of the occurrence of persistent large-scale disruptions patterns in the global circulation of the atmosphere (Wilhite and Svoboda, 2000). Once a drought is initiated it can be maintained by regional and local atmospheric processes, as well as by local hydrology, land cover, and groundwater feedbacks. On the other hand, vulnerability and exposure to drought varies spatially and is independent of drought occurrence.

Vulnerability is determined by social factors such as population demographic characteristics, technology, policy, social behaviour, land use patterns, water use, economic development, diversity of economic base, and cultural composition. If these factors change over time, so vulnerability will. Subsequent droughts in a same region can have different effects, even if they are identical in intensity, duration, and spatial characteristics, since they are determined by the societal characteristics. The existence of an early warning system is an important coping capacity to reduce the impact of drought.

Drought properties, such as intensity, duration and spatial coverage were analysed in detail in Deliverable 6.3 both at Pan-African and case study level. Several global and continental datasets based on re-analysis, gridded observation, and remote sensing data were tested. A set of indicators, including Standardized Precipitation index (SPI), Standardized Precipitation-Evaporation Index (SPEI), Standardized Run-off index (SRI), Soil Moisture Anomalies (SMA) were evaluated. The indicators analysed at continental level showed a good agreement in North West and Southern Africa, while a lower agreement was observed in Central Africa. SPI calculated using remote sensing estimations (TRMM) also shows a good agreement with ECMWF ERA-I reanalysis in east Africa, including the Great Horn of Africa. The estimations of the indicators over Central Africa reflect the high uncertainty present in all precipitation datasets analysed.

An approach to drought vulnerability assessment was developed in deliverable 3.2. This report examines African patterns of drought vulnerability by mapping several drought-related indicators. The primary concerns of drought vulnerability in Africa are largely related on issues of food security and nutritional needs of the population, water supply and environmental degradation. This kind of vulnerability affects directly the development process of many countries.

According to data collected in deliverable D2.2, during the 2004/06 period widespread severe drought conditions were observed in Kenya, Rwanda, and Tanzania, where more than 7.2 million of people were affected by a low agricultural production, depletion of water sources, and famine. During the 1991/92 drought in Southern Africa, referred as the “apocalypse drought”, the total number of people affected was around 86 million, with 20 million considered to be at serious risk of starvation. During this event, the rain failed or was late across the region causing that grain yields in the ten states of the Southern Africa Development Community (SADC) were 56% of normal production (Green, 1993).

The risk associated with drought episodes in this report was considered taking into account the drought hazard and the drought vulnerability at the country level, although a specific risk map was also calculated at the water basin level. Although a case study at regional level should have been conducted for the Great Horn of Africa this was postponed and will be included in deliverable 6.2.

2. DROUGHT HAZARD DEFINITION

Drought hazard may be defined as a source of potential harm, a situation with the potential to cause damage or a threat or condition with the potential to create loss or damage to lives or to initiate any failure to the natural, modified or human systems. According to this, the hazard of a damaging event would be the probability of having to face in a given period drought conditions stronger than the maximum perturbation that can be accepted without significant damages (coping capacity).

Drought hazard is a highly complex phenomenon, the characterization and definition of drought is not straightforward, and multiple approaches can be followed to characterize droughts. However, the connection between different variables such as precipitation, infiltration, evapotranspiration, and runoff are difficult to model and represent. Different approaches using different indicators or thresholds can lead to different drought status. This difference is mainly driven by the complex interaction between the components of the hydro-climate system; moreover, from the point of view of end-users the meaning of drought is related with its impacts that may vary depending on the socio-economic system. For instance, the rain failure in a single month of the rainy season at a certain location could affect rainfed crops while the existence of water reservoirs in the same region would prevent irrigated crops to be affected.

2.1 STANDARDIZED PRECIPITATION INDEX (SPI)

The Standardized Precipitation Index (SPI) was developed by McKee et al. (1993, 1995) to provide a spatially and temporally invariant measure of the precipitation deficit (or surplus) for any accumulation timescale. It is computed by fitting a parametric Cumulative Distribution Function (CDF) to a homogenized precipitation time-series and applying an equi-probability transformation to the standard normal variable. This means the SPI is expressed in units of number of standard deviations from the median.

Typically, the gamma distribution is the parametric CDF chosen to represent the precipitation time-series (e.g. McKee et al. 1993, 1995; Lloyd-Hughes and Saunders 2002; Husak et al. 2007) since it has the advantage of being bounded on the left at zero and positively skewed (Thom 1958; Wilks 2002). Moreover, Husak et al. (2007) have shown that the gamma distribution adequately models precipitation time-series in roughly 98% of locations over Africa. In this study we use the Maximum-Likelihood Estimation (MLE) method to estimate the parameters of the gamma distribution.

A reduction in precipitation with respect to the normal precipitation amount is the primary driver of drought, resulting in a successive shortage of water for different natural and human

needs. Since SPI values are given in units of standard deviation from the standardized mean, negative values correspond to drier periods than normal and positive values correspond to wetter periods than normal. The magnitude of the departure from the mean is a probabilistic measure of the severity of a wet or dry event (Table 2-1).

Since the SPI can be calculated over different rainfall accumulation periods, different SPIs allow for estimating different potential impacts of a meteorological drought:

- SPIs for short accumulation periods (e.g., SPI-1 to SPI-3) are indicators for immediate impacts such as reduced soil moisture, snowpack, and flow in smaller creeks;
- SPIs for medium accumulation periods (e.g., SPI-3 to SPI-12) are indicators for reduced stream flow and reservoir storage; and
- SPIs for long accumulation periods (SPI-12 to SPI-48) are indicators for reduced reservoir and groundwater recharge

The exact relationship between accumulation period and impact depends on the natural environment (e.g., geology, soils) and the human interference (e.g., existence of irrigation schemes). In order to get a full picture of the potential impacts of a drought, SPIs of different accumulation periods should be calculated and compared. A comparison with other drought indicators is needed to evaluate actual impacts on the vegetation cover and different economic sectors.

Definition of SPI classes	
SPI ≤ -2	**Extremely dry**
-2 < SPI ≤ -1.5	**Severely dry**
-1.5 < SPI ≤ -1	**Moderately dry**
-1 < SPI ≤ 1	**Near normal**
1 < SPI ≤ 1.5	**Moderately wet**
1.5 < SPI ≤ 2	**Severely wet**
SPI > 2	**Extremely wet**

Table 2-1 Definition of Standard Precipitation Index (SPI) classes

The GPCC (Global Precipitation Climatology Centre) dataset was selected for the analysis. A comprehensive description and comparison between different global datasets and drought indicators can be found in DEWFORA D6.3 and Naumann et al. (2012). GPCC gridded dataset relies only in station data and covers more than one century of data. However, due to possible inhomogenities caused by changes over time in the number and spatial coverage of the stations used, only the period 1959-2010 was used in the present study.

2.2 UNIVARIATE ANALYSIS FOR DROUGHT CHARACTERIZATION

Having selected SPI as the drought indicator to be used, drought can be defined as a period in which the SPI itself is continuously below a certain threshold (Table 2-1). However, definition of the time scale is required for any specific evaluation since its impacts on different socio-economic systems are dependent on its definition.

Figure 2-1 is a frequency map showing the probability of having SPI below -1 during 1990-2010 for different aggregation periods (3, 6, 9, and 12 months). Here only small differences are observed mostly in the Sahel where meteorological and agricultural droughts (based on SPI3) are more likely when compared with other aggregation periods. Conversely, in central Africa (e.g. in D.R. Congo) more frequent hydrological droughts are associated with SPI9 and SPI12. Moreover, there exists low frequency oscillations related to drought occurrence and severity. This means that the drought hazard definition is dependent on the aggregation period analysed.

Decadal variability of rainfall in Africa during the 20th century was studied by several authors (Nicholson 1994; Hulme 1996; Moron 1997; Nicholson et al 2000; Nicholson 2001; Kruger 2006; Kane 2009). Relatively dry conditions in the early 20th century were clear in most of the continent with exceptions in equatorial East Africa and the areas with a Mediterranean climate. In West Africa relatively wet conditions were observed during the 1920s and 1930s, but relatively dry conditions persisted in much of southern Africa.

The 1940s were characterized by a widespread drought, particularly in West Africa, followed by more extreme fluctuations in the latter half of the 20th century (Nicholson 2001). The 1950s were probably the wettest period since at least the 1870s and 1880s for the whole continent, but a pattern of sub-normal rainfall prevailed in the equatorial regions. In the early 1960s the rainfall increased dramatically throughout most of the equatorial region. By the 1970s, increased dryness was widespread, especially in the early 1970s (Nicholson 1994), but the decade as a whole was relatively wet in much of southern Africa, a result of several years of extremely high rainfall in mid-decade. By the 1980s, rainfall was below the long-term mean over most of Africa, a trend that has continued into the 1990s.

The changes in the drought frequencies are analysed in Figure 2-2 and Figure 2-3. The well-known dry period that starts in the middle 1970's in the Sahel and West Africa leads to a higher drought frequency in these regions during the period 1970-1989. Another singularity is the low drought frequency in the Central Africa during the 1970-89 period followed by a significant increase in drought occurrence in the following 20 years. In that region a hydrological discontinuity (start of a dry period) during the 1970s was detected at almost all the basins in the region (Laraque et al 2001). In particular for the Congo River at the beginning of the 1980s the regime experienced a significant drop in the run-off (around 10%)

and continued right up until early 2000 with a drop in its interannual discharge of 10%. However for rainfall the change is not as evident as depicted by Conway et al 2009. The authors didn't found consistent signals in rainfall and river flows across the whole of the region. Central Africa shows very modest decadal variability, with some similarities to the Sahel (dry period starting during mid-1970s). However care is required in the interpretation of time series and secular variations using global datasets because some basins have a very low stations density . For instance, at the Congo basin there are a maximum of five gauges across $3.5x10^6$ Km^2 (Conway et al., 2009).

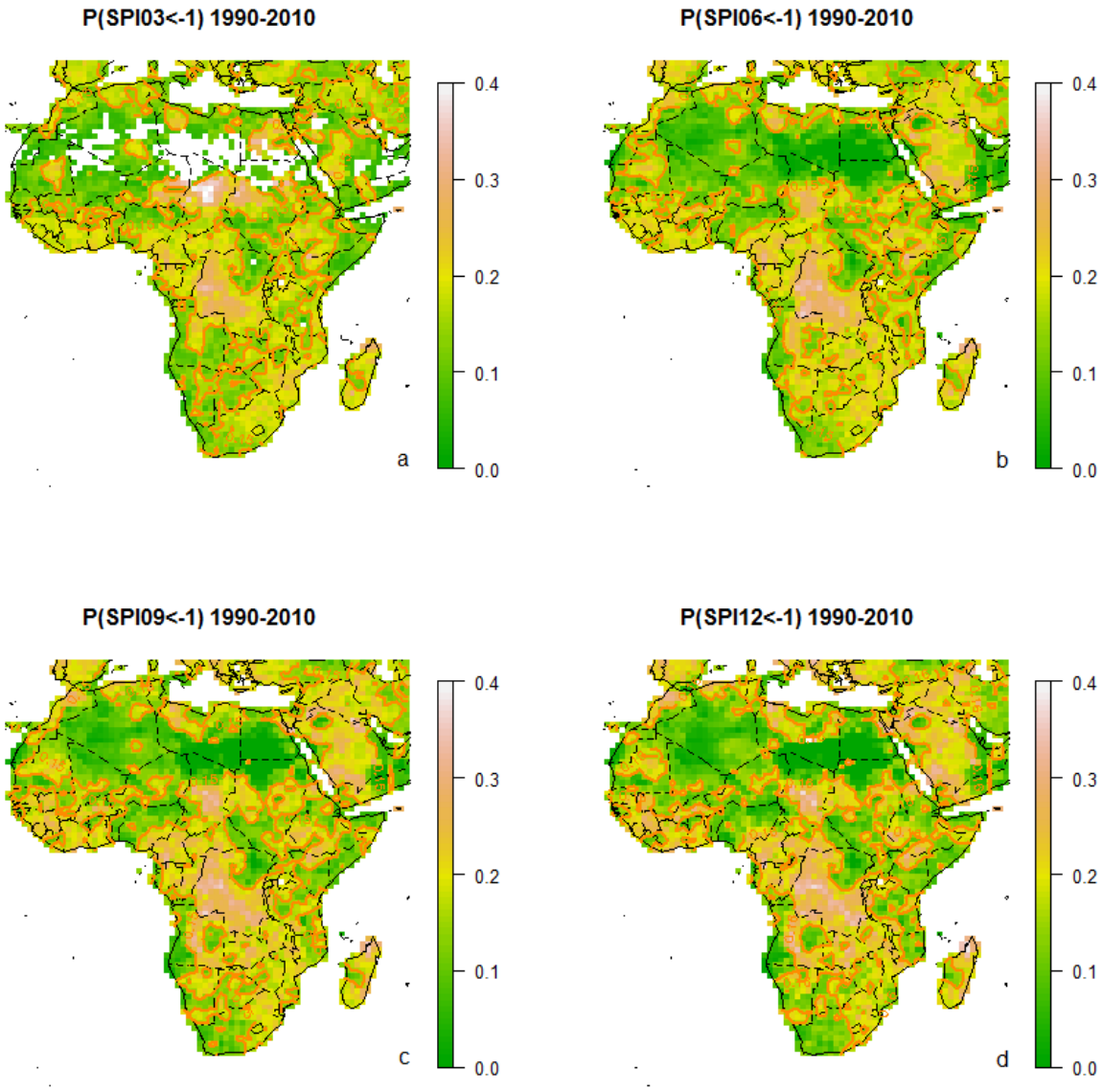

Figure 2-1 Relative frequency of SPI_k < -1 (k:3, 6, 09, 12 months) during 1990-2010.

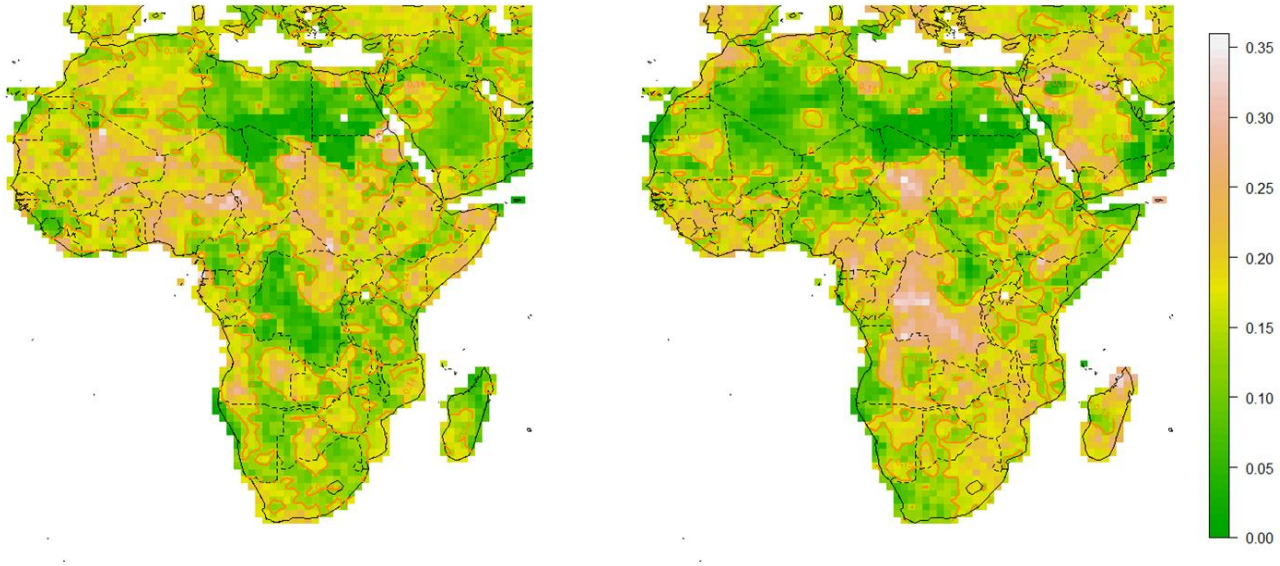

Figure 2-2 Comparison of the relative frequency of SPI06 < -1 for 1970-1989 (left) and 1990-2010 (right)

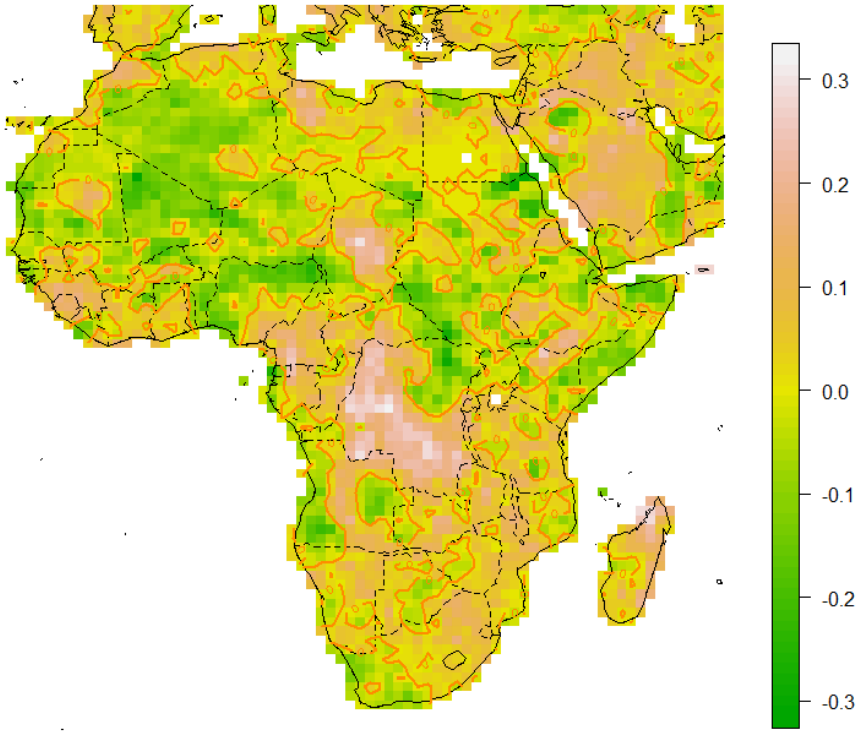

Figure 2-3 Differences between SPI06 <-1 frequencies in 1990-2010 and1970-1990

In order to take in account different potential impacts of meteorological droughts, an average of the relative frequency over different aggregation periods was calculated. Figure 2-4 shows the relative frequency of combined SPI below -1 aggregated at 3, 6, 9 and 12 months for the period 1990-2010. The general spatial extension of the regions under threat is similar to the

analysis for each single aggregation period (Figure 2-1). Only some differences are observed in the Sahel region, where meteorological droughts appear to have a higher frequency.

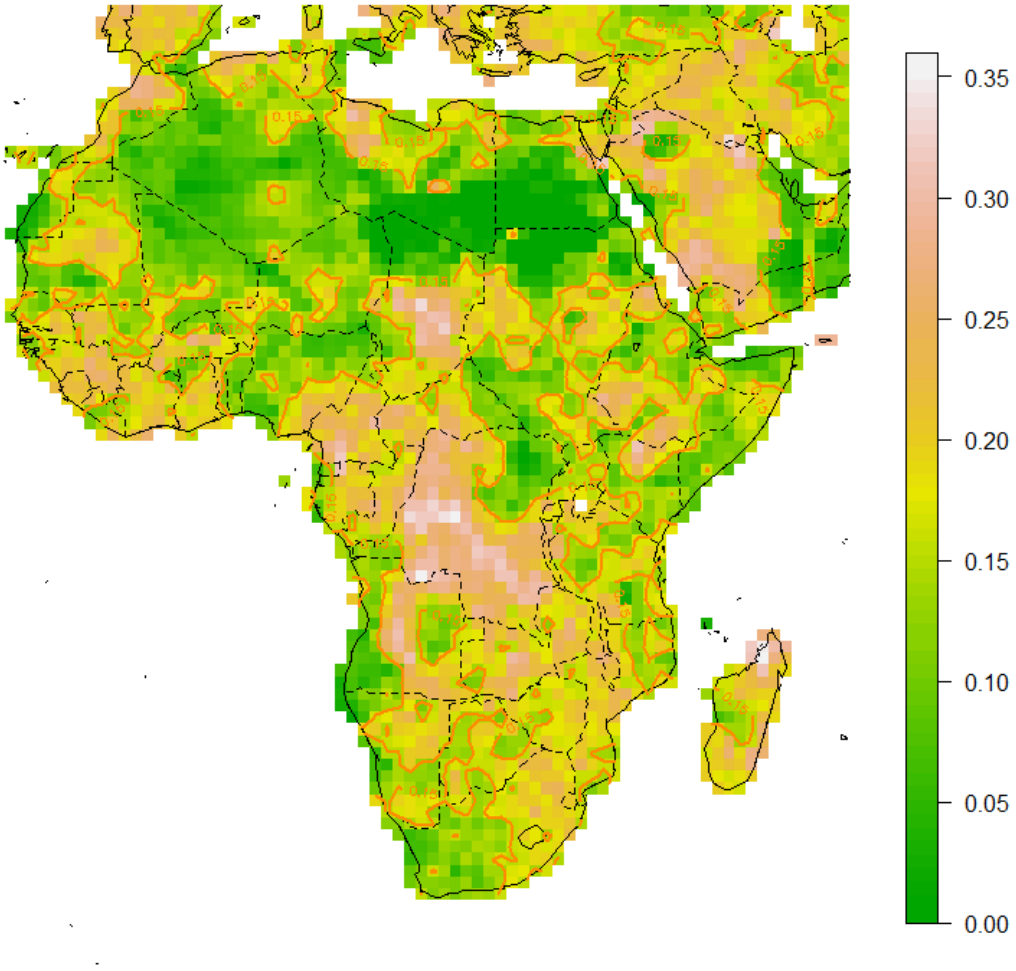

Figure 2-4 Relative frequency of combined SPI below -1 aggregated at 03, 06, 09 and 12 months for 1990-2010.

2.3 BIVARIATE ANALYSIS FOR DROUGHT CHARACTERIZATION

Due to complexity of drought hazard it can be argued that frequency alone is not sufficient to describe the level of hazard. In a more comprehensive way, drought phenomena may be described by their magnitude and duration together with the frequency of their occurrence.

In this section a bivariate approach to define drought hazard, using drought severity and duration derived from the SPI, is explained.

Each period with continuous negative SPI is defined as a drought event. Cumulative SPI values of a dry event are used to measure the severity of drought event and according with McKee (1993) is defined as:

$$\mathbf{S} = -\sum_{i=1}^{D} \mathbf{SPI}_i$$

2-1

Where S is the severity and D represents the drought duration in months of each dry event. Figure 2-5 shows a schematic representation of the S and D and the inter-arrival time between two dry periods. As these two variables are not independent a bivariate analysis could be assessed in order to better represent drought hazard. However, for most of the locations, duration and severity usually follow a different kind of marginal distribution. For this reason a copulas approach was used to link the marginal univariate distributions and finally obtain the bivariate joint probabilities of occurrence.

2.3.1 Copulas

Developed by Sklar (1959), copulas are functions that link univariate distribution functions to form multivariate distribution functions. The merit of using copulas to construct multivariate distributions is that copulas can separate the dependence effects from each marginal distribution. Construction of a multivariate distribution is thus reduced to studying the relations among the correlated random variables if marginal distributions are given.

Considering a situation with two random variables, Sklar's Theorem states that if $F_{D,S}$ (d, s) is a two-dimensional distribution function with marginal distributions F_D(d) and F_S(s), then there exists a copula C such that

$$F_{D,S}(d,s) = \mathrm{C}(\mathrm{F}_D(\mathrm{d}), F_S(\mathrm{s}))$$

2-2

Conversely, for any univariate distributions F_D(d) and F_S(s) and any copula C, the function $F_{D,S}$(d, s) defined above is a two-dimensional distribution function with marginal distributions F_D(d) and F_S(s). Furthermore, if F_D(d) and F_S(s) are continuous, then C is unique. The detailed proof of Sklar's Theorem can be found in Schweizer and Sklar (1983).

Under the assumption that the marginal distributions are continuous with probability density functions f_D(d) and f_S(s), the joint probability density function then becomes

$$F_{D,S}(d,s) = c(\mathrm{F}_D(\mathrm{d}), F_S(\mathrm{s}))f_D(d)f_S(s)$$

2-3

where c is the density function of C, defined as

$$c(u,v) = \frac{\partial^2 C(u,v)}{\partial u \partial v}$$

2-4

Several authors provided a number of one-parameter families of copulas (Joe, 1997; Frees and Valdez, 1998; Nelsen, 2006; Cherubini et al., 2004). Copula functions were already tested for assessing the multivariate nature of droughts (Nelsen, 2006; De Michele and Salvadori, 2003; Salvadori and De Michele, 2004; Kao and Govindaraju, 2008; Lee and Salas, 2011). The bivariate joint distribution of drought characteristics, based on duration and severity, has been modeled with several copula functions and marginal distributions. Shiau (2006), Shiau et al. (2007), Lee et al (2012), and Shiau and Hsiao (2012) applied different types of copulas for the modeling of the joint distribution of drought duration and severity and fitted the exponential and gamma marginal distributions to drought duration and severity, respectively. Clayton, Frank, Gumbel and Gaussian copulas were tested in the present analysis. A more detailed description about the methodology can be found in appendix A.

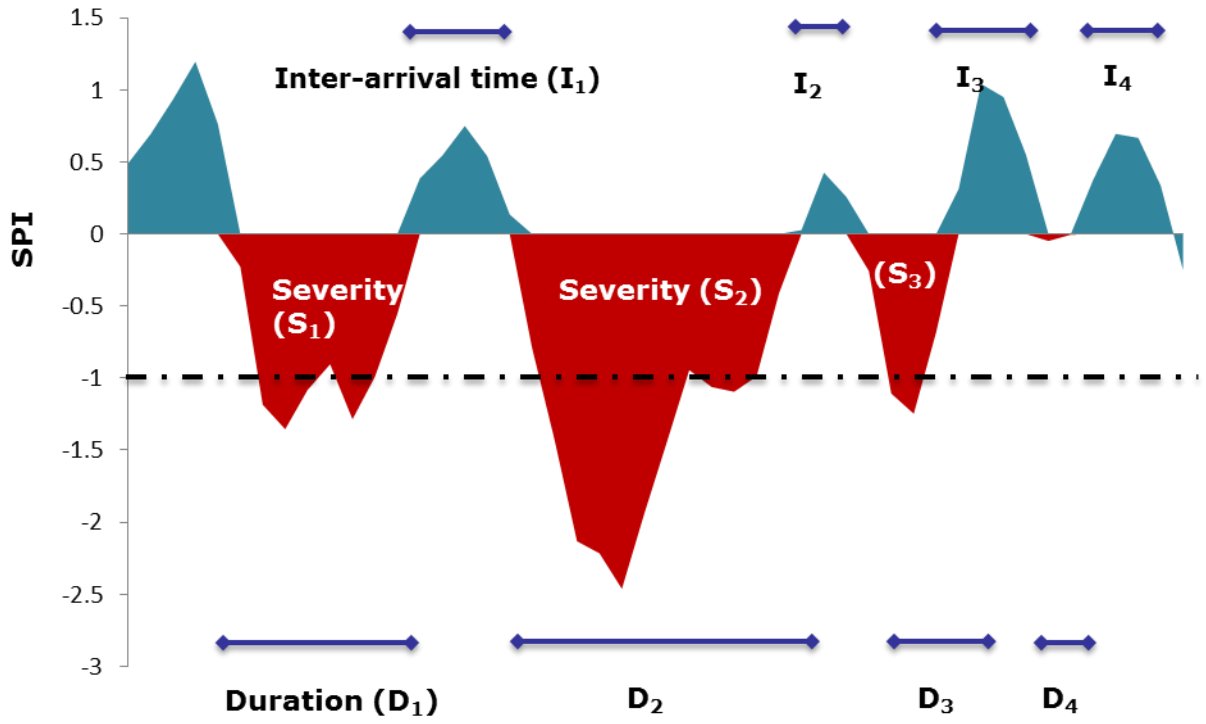

Figure 2-5 Schematic representation of drought Severity (S) and Duration (D) definitions using SPI.

As a first step to perform the Copulas analysis several univariate distributions for drought duration (D) and severity (S) were tested at continental level. Weibul, Gamma, Kernel and exponential distribution where tested for the D while Weibul, Kernel and Gamma were assessed for S.

Figure 2-6 shows the different distributions fitted for one single pixel at the Limpopo Basin. In general both variables are characterized by an exponential decaying in the frequency while both severity (S) and duration (D) of droughts increase. The distributions that best fit at continental level for S and D are the Gamma distribution (89 % of the pixels) and the exponential distribution (69% of pixels) respectively.

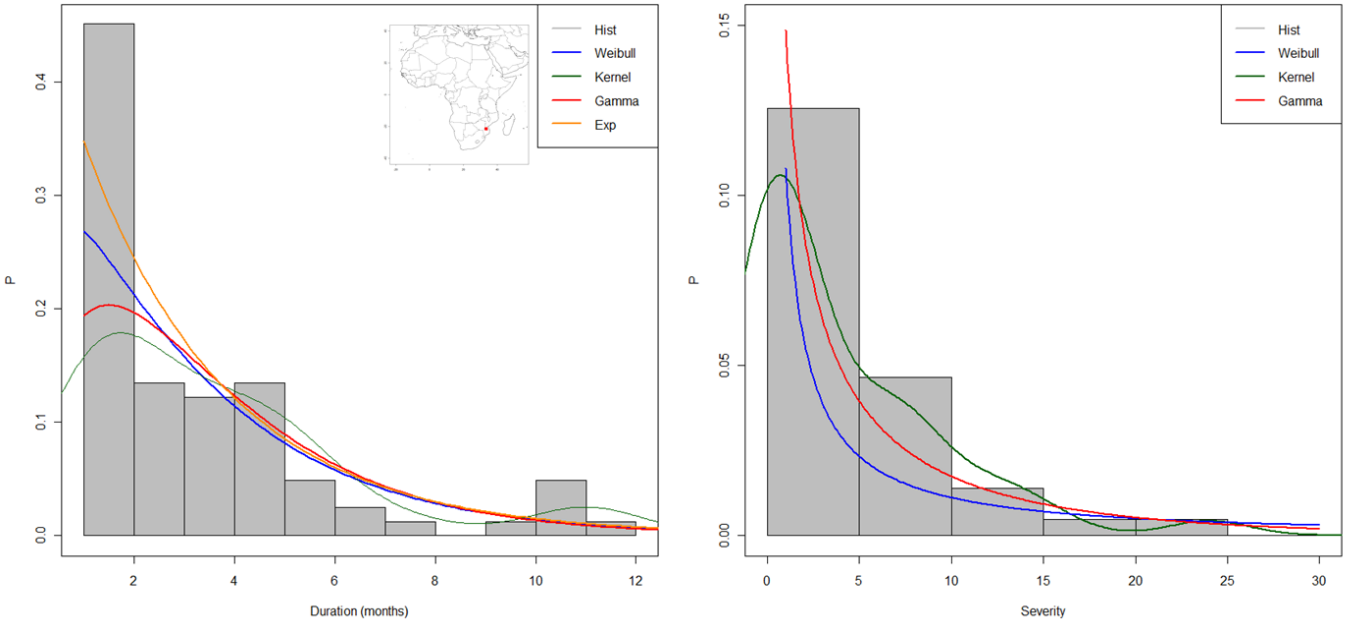

Figure 2-6 Marginal empirical and theoretical distribution of drought Duration and Severity for a single pixel in the Limpopo basin (long: 33.5, lat: -21.5).

For most of the applications in drought management and decision making, knowledge of joint occurrence of different drought characteristics is helpful to define the maximum departure from normal conditions that can be accepted without significant damages or loses (coping range). Five different families of copulas (Clayton, Frank, Gumbel, Gaussian, and empirical) were tested in order to assess their fitness to the observed data. Figure 2-7 shows the joint CDF and PDF for different Copulas. Small differences are observed for the lower joint severity-duration values while these differences increase for joint extreme events.

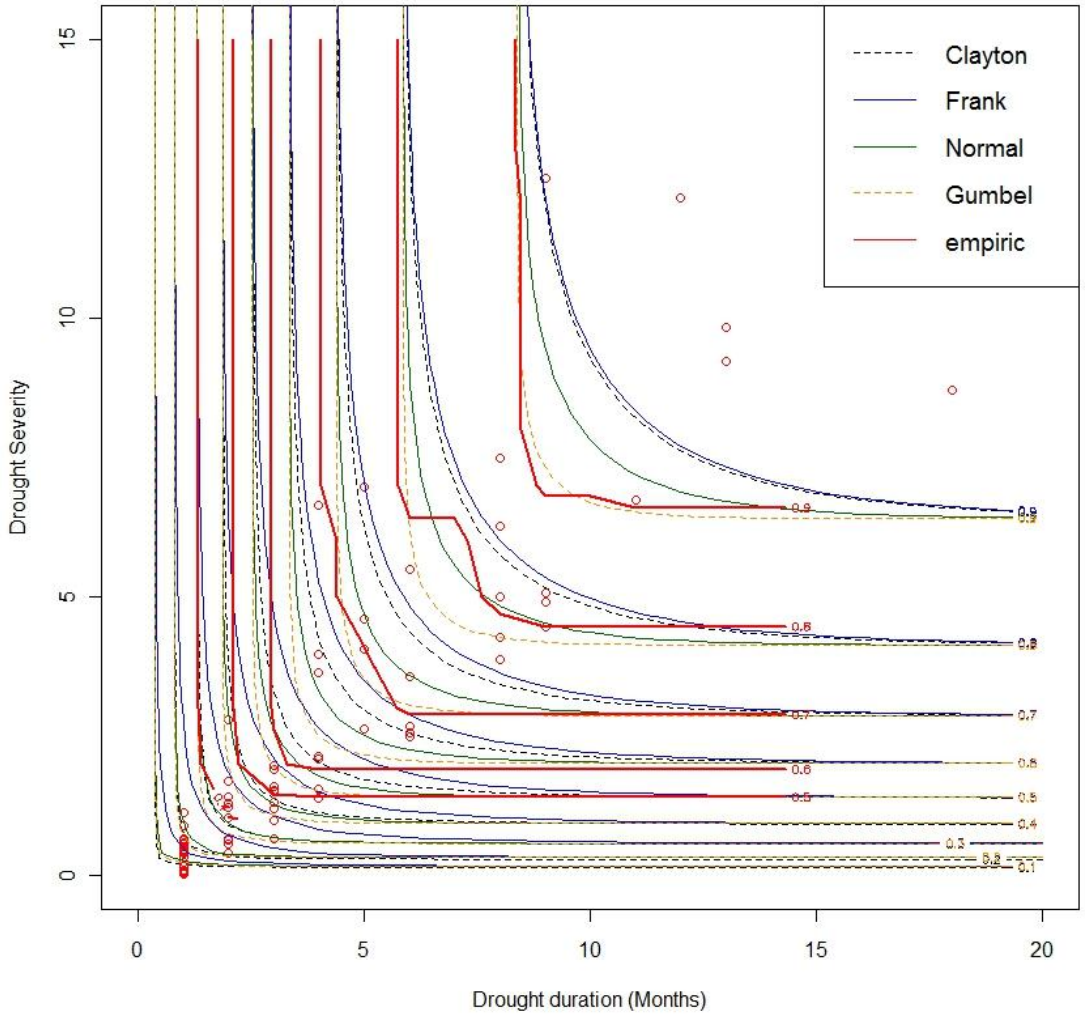

Figure 2-7 Joint probability of drought duration and severity for a pixel in Mozambique using GPCC data (1959-2010) for different copulas.

Fitting copulas to empirical observations is still an open problem in Statistics and several Goodnes-of-Fit procedures have recently been proposed. At present the most feasible and realistic solution is represented by multivariate Goodness-of-Fit tests based on the empirical copula process (Genest et al 2009; Berg 2009; AghaKouchak et al 2013).

In order to show the agreement between observations and the Frank Copula the joint probability under certain thresholds was calculated. Figure 2-8 shows empirical and theoretical joint probabilities P(D≤ i, S≤ i) with i=1,2…, 10. Empirical joint probabilities were calculated as

$$P(d \leq i, s \leq i) = \frac{F(D,S)}{N}$$

2-5

where F(D,S) are number of pairs of D≤ i and S≤ i and N is the sample size. An overall good agreement is observed between the joint probabilities even for the extremes values where the theoretical approach tends to overestimate the probabilities.

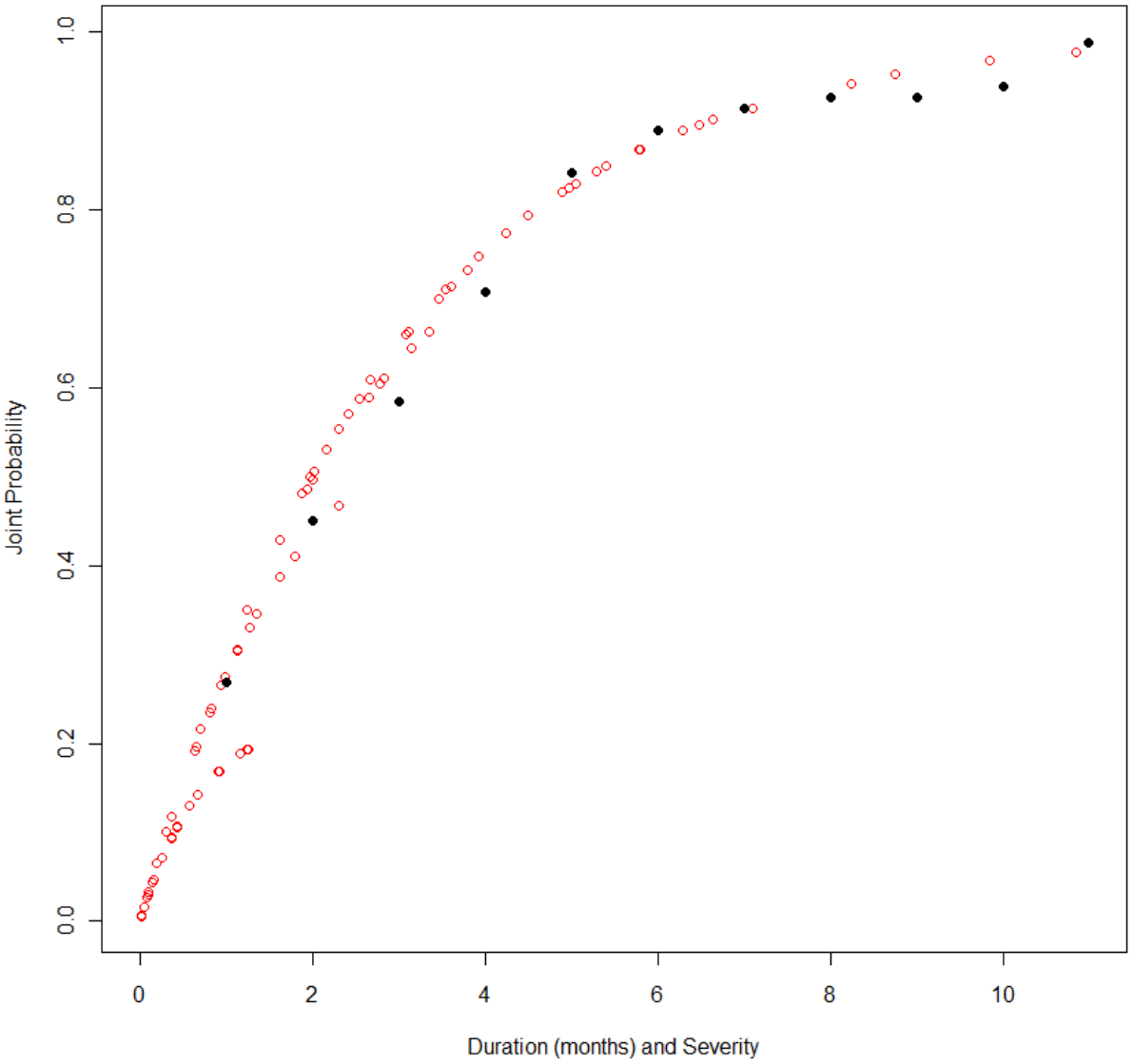

Figure 2-8 Empirical and theoretical joint probability of duration and severity of droughts (Frank Copula).

To represent overall impacts of droughts, the sum (P) of joint probabilities of all dry events for each pixel is used. It is based on the idea that higher occurrence of droughts events with greater severity or duration have greater potential impacts on the system.

$$P = \sum P(d,s) \qquad 2\text{-}6$$

Where P(d,s) is the joint probability of an observed drought event with a duration of d_i and a severity of s_i.

Then taking into account the maximum and minimum values of the summed probabilities, the values of P are rescaled to have values rangeing between 0 and 1 (Shiau and Hsiao, 2012):

$$DHI(k) = 1 - \frac{(\max(P) - P_k)}{\max(P) - \min(P)} \quad 2\text{-}7$$

where DHI(k) represents the drought hazard index for the k^{th} pixel.

Figure 2-9 shows the values of DHI estimated using SPI 12 for each pixel. If this DHI is overlaid with the Köppen-Trewartha eco-zones (Figure 2-11, FAO, Global Forest Resources Assessment, 2000) some similarities can be observed; for example, the main desert areas characterized by a hot and arid climate (Sahara and Kalahari) are associated with low values of drought hazard. This feature is also observed in the Tropical moist deciduous forest zones in Central Africa (mainly in Angola, Zambia and South D.R of Congo) where the region is characterized with an overall low probability of drought occurrence.

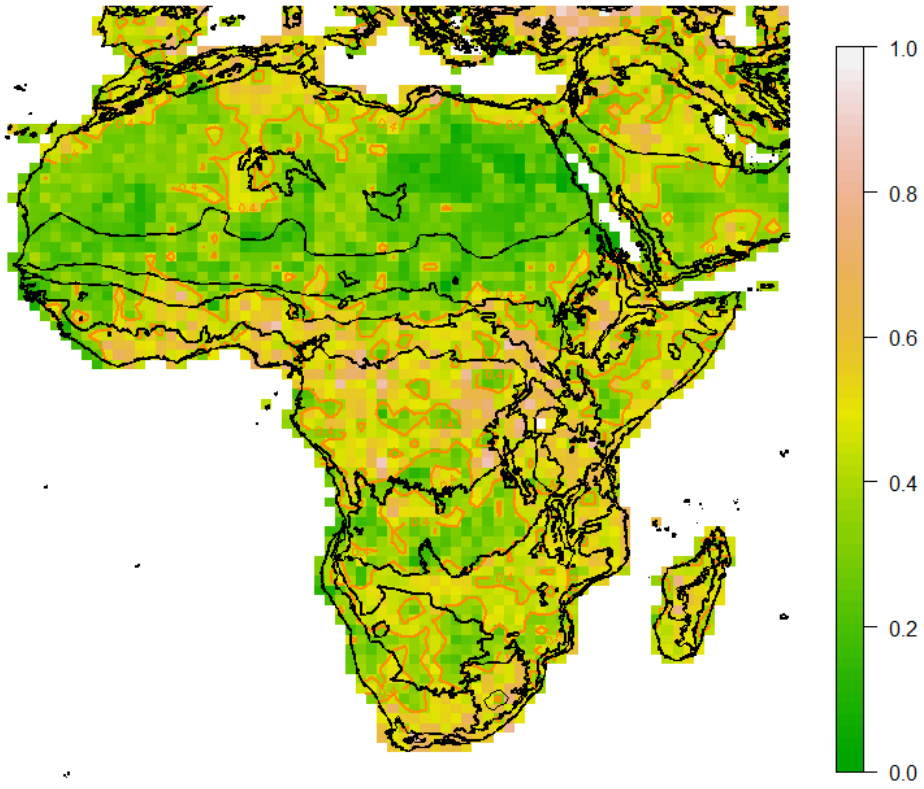

Figure 2-9 DHI based on SPI 12 and FAO ecozones.

On the other hand, the Mediterranean coast of Africa which is associated with a markedly dry summer, equatorial regions with a dry winter, the Sahel, southern east Africa, and the wet part of Southern South Africa are more drought prone than other regions.

However, using a certain aggregation period for computing SPI (like in the previous example) shows only a partial feature of the drought characterization, since for example SPI-12 will be more related with hydrological droughts. In order to combine the different effects of different types of droughts, a combined drought hazard index calculated by using SPI aggregated by 3, 6, 9 and 12 months is introduced. Figure 2-10 shows the comparison between DHI using SPI 12 and the combined DHI. Almost similar results are observed, but larger areas in the tropical rainforest seem to be now less drought prone due to less meteorological and seasonal droughts. Moreover, the northern border of the Sahel tends to show higher DHI values mainly due by the occurrence of seasonal droughts.

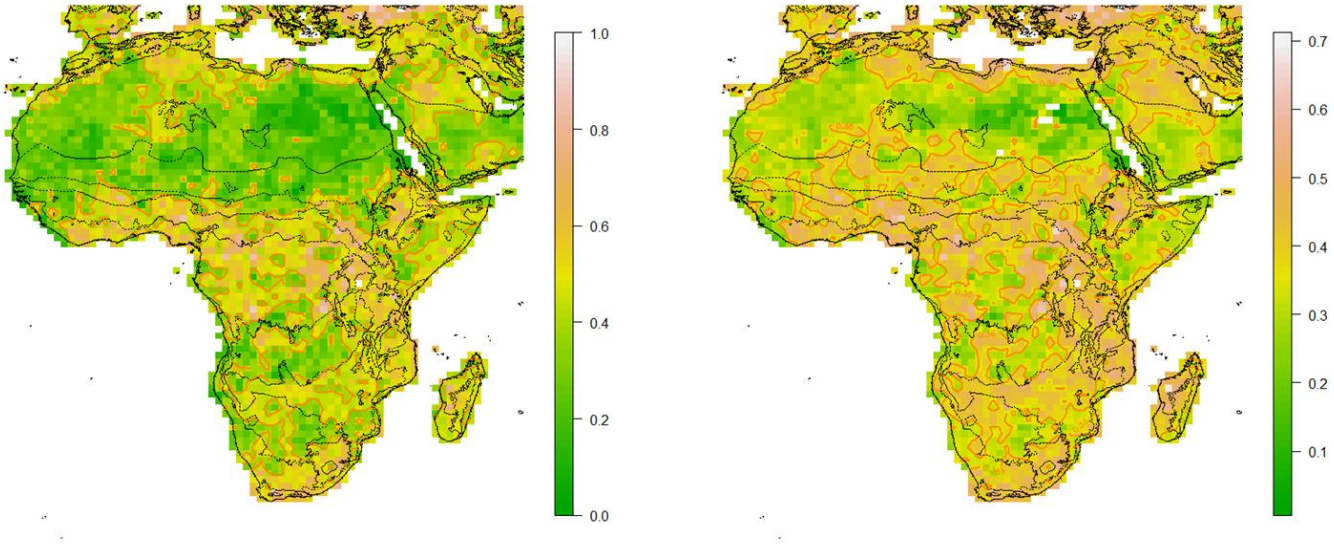

Figure 2-10 DHI-12 (left) and sum of DHI for 03, 06, 09 and 12 months (right). In black dashed lines are representing the FAO eco-zones.

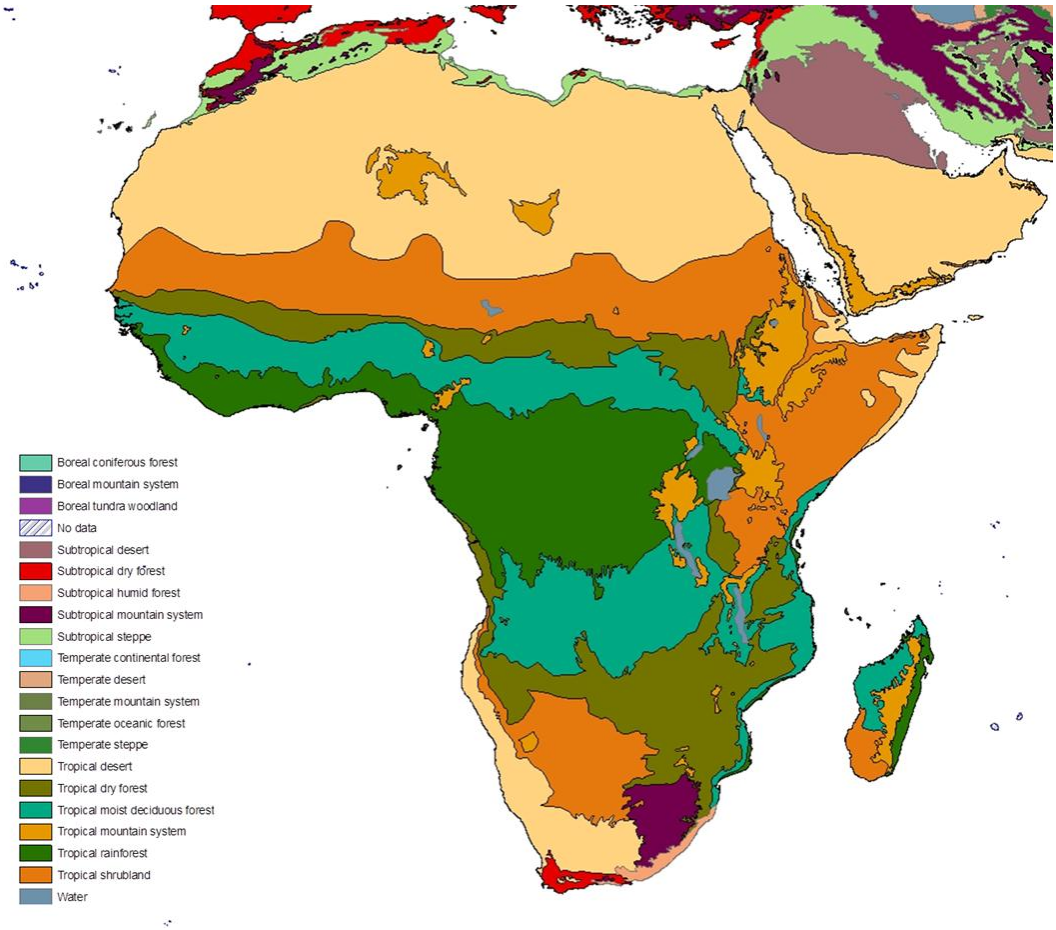

Figure 2-11 Köppen-Trewartha Africa ecological zones. Source (FAO FRA 2000)

3. DROUGHT VULNERABILITY ASSESSMENT

In order to assess the drought risk for a certain region definition of vulnerability to drought should reflect the complex interactions between the socio-economic systems and the physical environment. Defining vulnerability to drought is complex and involves some measure of susceptibility, exposure, coping capacity and adaptive capacity (Birkmann, 2007; Iglesias et al., 2009).

A suite of socio-economic indicators may be used as proxies to characterize drought vulnerability. Ideally, the indicator values may define thresholds. However, definition of critical thresholds is very complex. A threshold is the value at which action is initiated – and not necessarily that at which problems occur. In some literature this leads to two types of threshold – the one is called an action or operational threshold, the other a result threshold.

This section follows the methodologies proposed in D3.2 for the case studies and in the Pan-Africa case study. Under this scoop, drought vulnerability incorporates natural and social aspects. Moreover, in the appendix D a vulnerability and risk study was performed in Kenya using local data.

3.1 DROUGHT VULNERABILITY INDEX (DVI)

The Drought Vulnerability Index (DVI) can be applied locally or spatially and with different aggregation levels of the input data. The intermediate components can be evaluated independently, allowing comprehensive interpretation of the strengths and weaknesses of each system. The sequential steps taken for the quantification of the DVI are: (a) select variables that are relevant; (b) normalize the variable values with respect to some common baseline; (c) combine the sub-component variables within each category by weighted averages; and (d) quantify DVI as the weighted average of the components. The scores of the DVI range on a scale of 0 to 1, with the total being generated as the average of each component.

Table 3-1 shows the components and sources of the DVI. The DVI is a composite indicator calculated by weighted aggregation of 15 socio-economic factors. The factors were included because data availability and the variables are drought scenario dependent and geographically explicit. This vulnerability index may be used to understand the sensitivity of the system and to assist in the selection of measures to be adopted.

The DVI is calculated with a similar methodology as the Human Development Indicator (HDI). Each component of the DVI can be viewed as a dimension. Before calculating the overall DVI, an indicator for each of the dimensions needs to be computed. The four dimensions were named as Renewable Natural Capital, Economic Capacity, Human and

Civic Recourses and Infrastructure and Technology. All of these categories contain multiple indicators and were aggregated using equal weights.

Indicator	Source	Type
Renewable Natural Capital		
Agricultural water use (%)	Aquastat	V
Total water use (% of renewable)	Aquastat	V
Average precipitation 61-90 (mm/year)	Aquastat	A
Irrigated area (% of cropland)	Aquastat	A
Population density (inhab/km^2)	Aquastat	V
Economic capacity		
GDP per capita US$	UNDP (HDI)	A
Agricultural value added/GDP %	Aquastat	V
Energy use (Kg oil equivalent per capita)	World Bank	V
Population living below $1.25 PPP per day (%)1$/day	UNDP (HDI)	V
Human and Civic Resources		
Institutional capacity	DEWFORA WP 2.0 to 1	A
Adult literacy rate (%)	UNDP (HDI)	A
Life expectancy at birth (years)	UNDP (HDI)	A
Population without access to improved water (%)	World Bank	V
Infrastructure and technology		
Fertilizer consumption (kilograms per hectare of arable land)	World Bank	A
Water infrastructure (storage as proportion of total RWR)	Aquastat	A

Table 3-1 Vulnerability factors and their related weights included in the DVI. Each indicator is flagged as V (vulnerable) and A (adaptive) depending if tis positive or negative correlated with the overall vulnerability.

To compute the dimension indicators, minimum and maximum values are chosen for each underlying variable. These minimum and maximum values are used to harmonize the DVI and refer to the minima and maxima of the areas which are the in the scope of analyzes. Performance in each dimension is then calculated as the dimension indicator with;

$$V_i = \frac{X_i - X_{min}}{X_{max} - X_{min}} \quad 3\text{-}1$$

for proxies which exhibit a positive correlation to the overall vulnerability, and with

$$V_i = 1 - \left(\frac{X_i - X_{min}}{X_{max} - X_{min}}\right) \quad 3\text{-}2$$

for proxies which exhibit a negative correlation.

Here X_i represents the proxy value for country i, X_{min} the minimum of the values in the sample, and X_{max} the maximum of the values in the sample. Then each dimension (D) is computed as the weighted aggregation of the proxies that define the dimension.

The overall Drought Vulnerability Index is then calculated as a weighted aggregation of the dimension indices as;

$$DVI_i = \sum_{i=1}^{n} W_i D_i$$

3-3

Where W_i are the weights assigned for the i dimension (with i=1,…,n). Then the DVI gives the relative vulnerability of a country in respect to the given countries.

In order to include a socio-economic indicator to the DVI, it must have at least half of the countries without missing data. After that from the 15 indicators selected, the amount of missing data for each ranges between 0% to 46% (Table 7-3). For the indicators that present missing values according to the main source (see table 3-1) but the data was available through other well-reputed sources, the values were completed. This is the case for the Energy use, GDP per capita and fertilizer consumption as depicted in table 3-2.

Indicator	Source
GDP per capita (US$)	World Statistics Pocketbook (United Nations Statistics Division)
Energy use (Kg oil equivalent per capita)	World Statistics Pocketbook (United Nations Statistics Division)
Fertilizer consumption (kilograms per hectare of arable land)	Fertilizer consumption total in Tons from Faostat
	Arable land in Kha from Aquastat

Table 3-2 Secondary sources of information used to construct the DVI. Note: The hyperlink to access the entire data are associated at each source name.

For most of the indicators the missing values ranges between 2% and 7%, however for the People living below poverty (PLP) this values is missing for the 46.3% of the countries and no other dataset was used to fill the gaps. This component was considered was considered in the analysis because the DVI is a combined theory and data based indicator, and in this framework this information is relevant to determining the social vulnerability, so when the data becomes available the DVI could be updated. Moreover a test by computing DVI with and without PLP was performed and not significant changes were observed in the overall DVI values (absolute maximum differences were around 0.03).

After the data completion only Comoros (2), Cape Verde (2), Djibouti (3), Equatorial Guinea (2), Libya (2), Sao Tome and Principe (3) and Seychelles (2) presents more than one missing indicator. For those countries the comparison must be done carefully.

The results for the DVI are presented in Figure 3-1 and Figure 3-2. According with this analysis the countries with the highest vulnerability are Somalia, Mali, Ethiopia, Niger, Burundi and Chad. In order to understand the source of vulnerability in each case it is useful to analyse each dimension and sub-index separately. For instance, Mali shows high vulnerability in Renewable Natural Capital and Human and Civic Resources, while Ethiopia and Somalia are vulnerable in the four sub-categories.

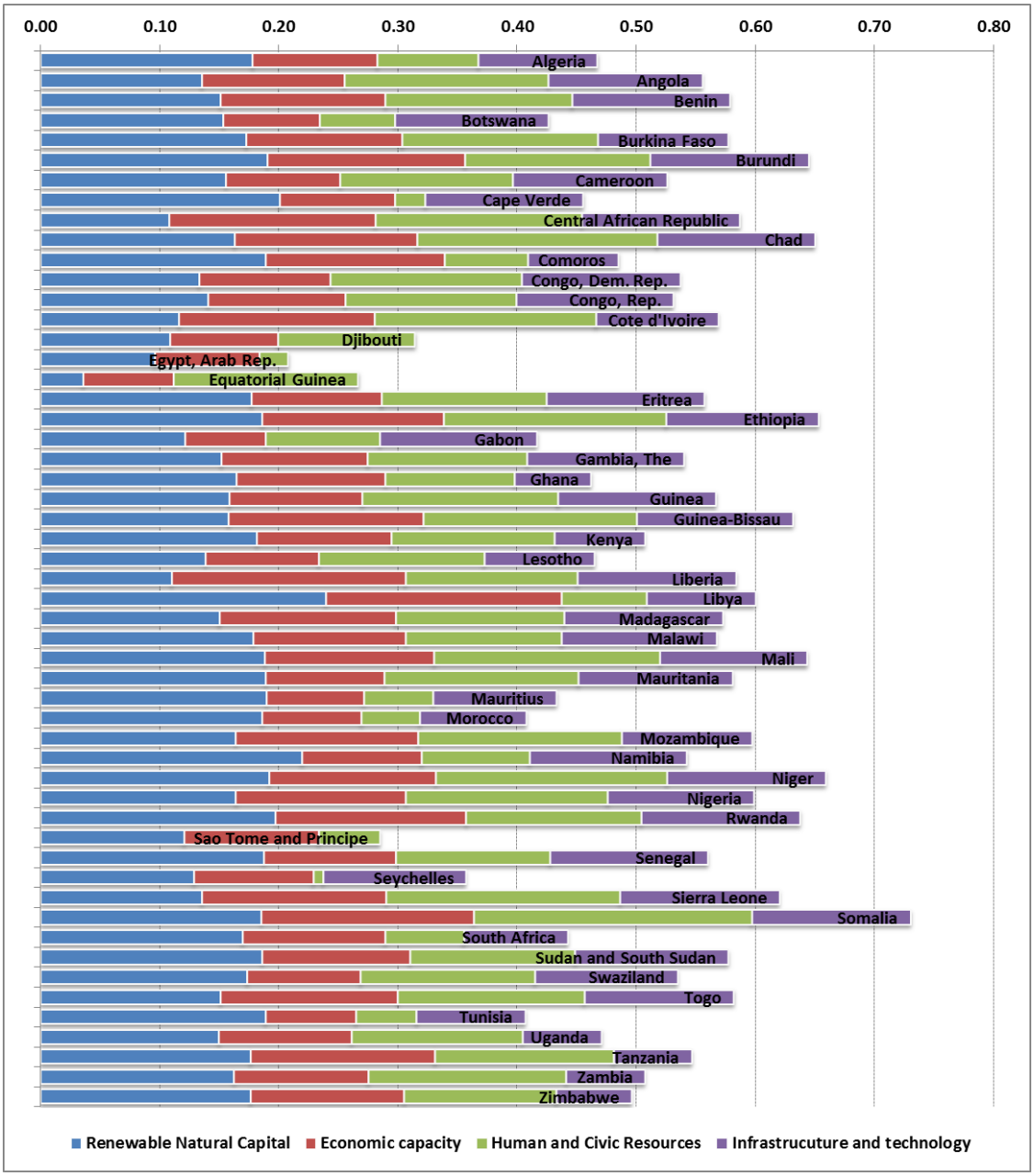

Figure 3-1 Four dimensions of DVI (Renwable Natural Capital, Economic capacity, Human and Civic Resourses and Infrastructure and technology).

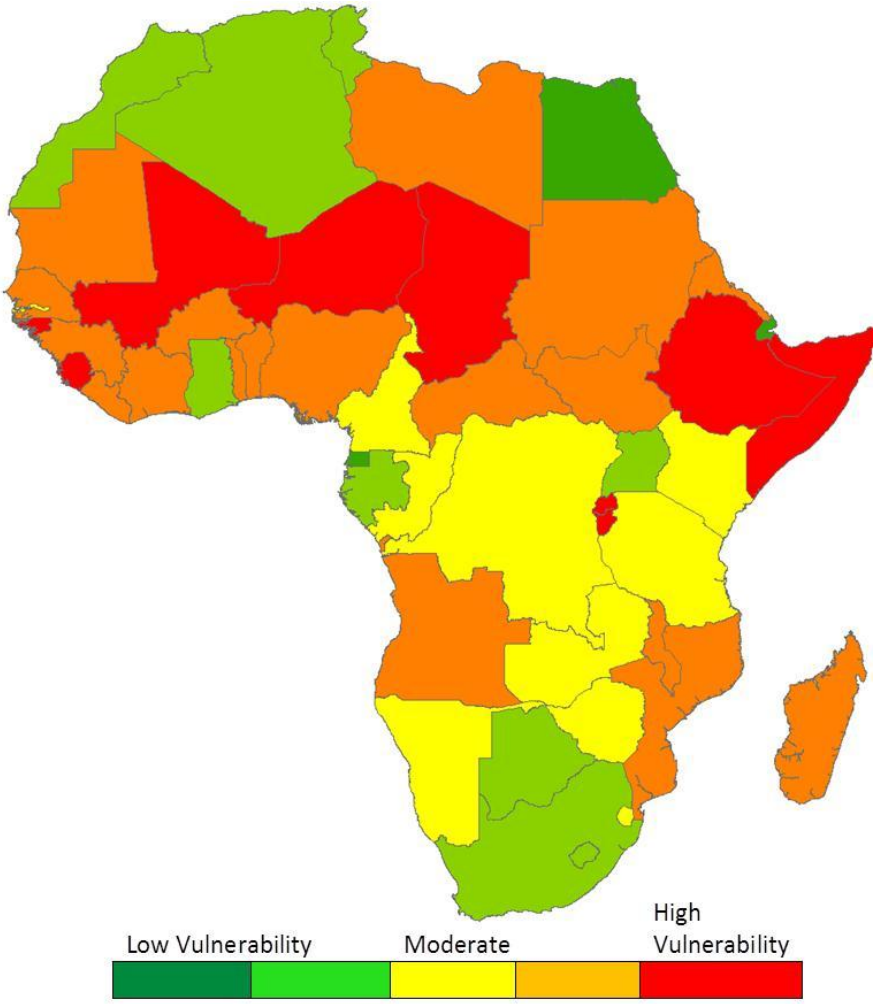

Figure 3-2 Drought vulnerability map at country level.

3.2 VULNERABILITY OF RENEWABLE NATURAL CAPITAL TO DROUGHTS (A PIXEL BASED ANALYSIS)

Using satellite-derived and land-based monitoring products the UNH Water Systems Analysis Group has developed a compendium of Earth System and socio-economic databases describing the current state of global water resources, including associated human interactions and pressures. This gridded datasets was analyzed at global scale for water scarcity studies (Vörösmarty et al. 2000). A recent study in Africa (Vörösmarty et al. 2005) demonstrates the utility of such geospatial data sets in a wide range of indicator applications in areas with scarce local data.

Between the variables present in this digital archive, irrigation-equipped area, irrigation water withdrawals, agricultural area, and rural and total population were tested in order to generate a drought vulnerability index of agricultural systems in Africa (Table 3-3).

Indicator
Irrigation-equipped area (km^2 per grid cell)
Irrigation water withdrawals (millions of m^3/year per grid cell)
Agricultural area (km^2)
Rural population, year 2000 (people per grid cell)
Total population, year 2000 (people per grid cell)

Table 3-3 Vulnerability factors used in the gridded data analysis. Source: World Water Assessment Program, World Water Development Report II. http://wwdrii.sr.unh.edu/index.html

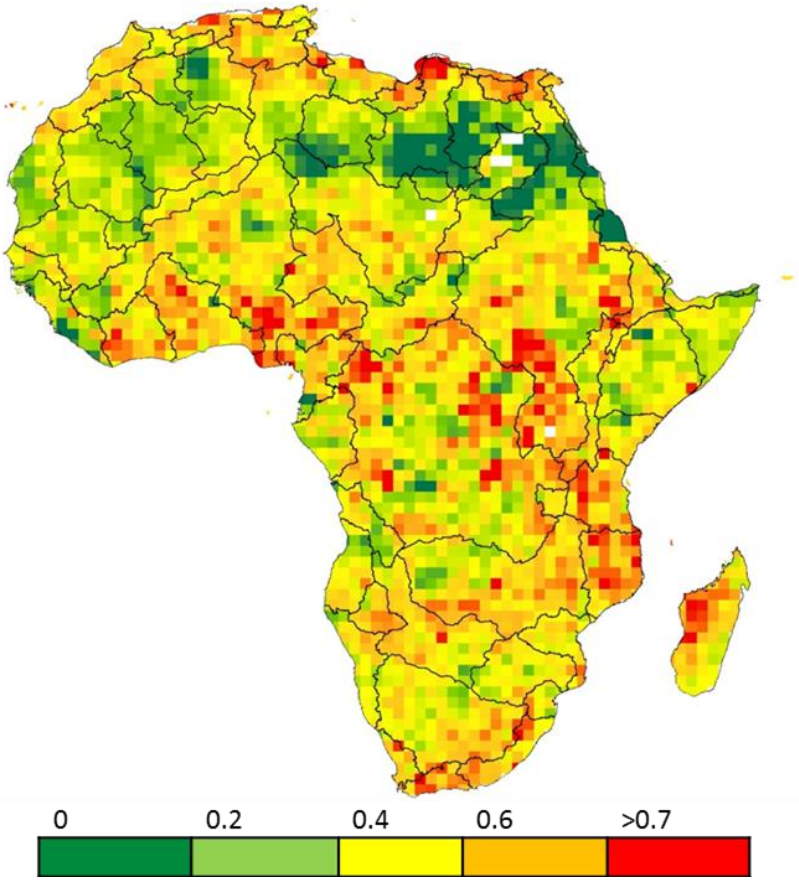

Figure 3-3 Drought Hazard Index clasified by quantiles.

Figure 3-4 shows the vulnerability of agricultural systems in Africa at pixel level. All the datasets of vulnerability indicators (0.5°x0.5°) were rescaled to fit the lower resolution (1°x1°) given by the hazard indicators (Figure 3-3). The areas with high density of crop areas and population are depicted as the more vulnerable. Those areas include the Mediterranean climates of Africa, the Sahel and almost the entire eastern part of the continent.

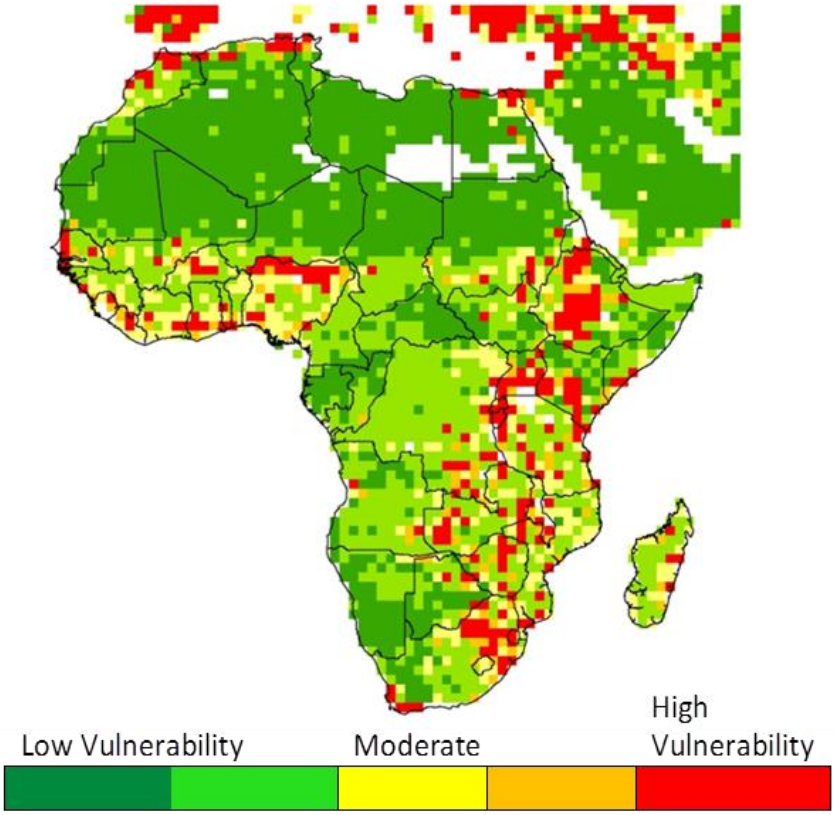

Figure 3-4 Drought vulnerability of agricultural systems

4. RISK ASSESSMENT

4.1 RISK ANALYSIS AND DEFINITION

Most of risk definitions rely on probabilistic definitions related to the probability of occurrence of a hazard that could trigger a disaster or negative events with undesirable outcome or the probability of a disaster estimated by the combination of the probability of a hazard event with the consideration of the likely consequences of the hazard (Brooks, 2003). However, several approaches to risk definition can be found in the literature. A synthesis of different risk definitions according different authors could be found in Brooks, 2003 (see Appendix A).

Risk defined as a function of hazard and social vulnerability is compatible with the risk definition as “hazard probability x consequence”, and also with risk defined in terms of outcome. The probability of an outcome will depend on the probability of occurrence of a hazard and on the social vulnerability of the exposed system, which will determine the consequence of the hazard.

The effect of a natural hazard on the objects or people of a particular area exemplify the complex interrelationships and emerging domino effects. The UN (1991) and the UNDP (2004) define a conceptual framework for risk assessment as follows:

$$\boldsymbol{Risk = Hazard\ x\ Vulnerability} \qquad \textit{4-1}$$

According to this definition, risk is related to the capacity of a society to cope, resist and recover from any certain impact (vulnerability) and the hazard is related with an external factor that will be defined by intensity of the natural phenomena that threat the social system (Bohle, 2001).

The hazard component in equation (4-1) is defined as the probability of a drought event happening in a certain period of time, taking into account different drought severities and durations for different aggregating periods (DHI). The second component, vulnerability, was conceptually defined as the relation of the exposure and the susceptibility as for a system with a defined coping capacity. In order to define the vulnerability of each region a Drought Vulnerability Index (DVI) was constructed by using several proxies that characterizes vulnerability at national, regional or pixel level.

According to this definitions risk was defined in this work as;

$$\boldsymbol{Risk = DHI\ x\ DVI} \qquad \text{4-2}$$

As a second step and in order to compute the risk maps at country level, the drought hazard must be aggregated from the original resolution. Taking a regional average of the data for each country will be translated in a loss of information. For instance, averaging a large country generally could not be representative of disasters that occurs locally. Moreover,

relatively wet and dry regions in the same country can neglect the drought hazard signal. For this reason, the risk maps were elaborated using the average and the maximum hazard for each country (Figure 4-1). According this, the countries that shows greater drought risk remains in the same group of categories for both analyses. For instance Sudan, Ethiopia, Mozambique, Tanzania, Chad, Nigeria and Mali remains as moderate high to high risk classes. In the other hand, Botswana, South Africa, Gabon, Morocco, Tunisia and Egypt remains in the low risk classes. The only significative change is observed in Togo where it changes to high risk area using the country average to low risk if the country maximum is considered.

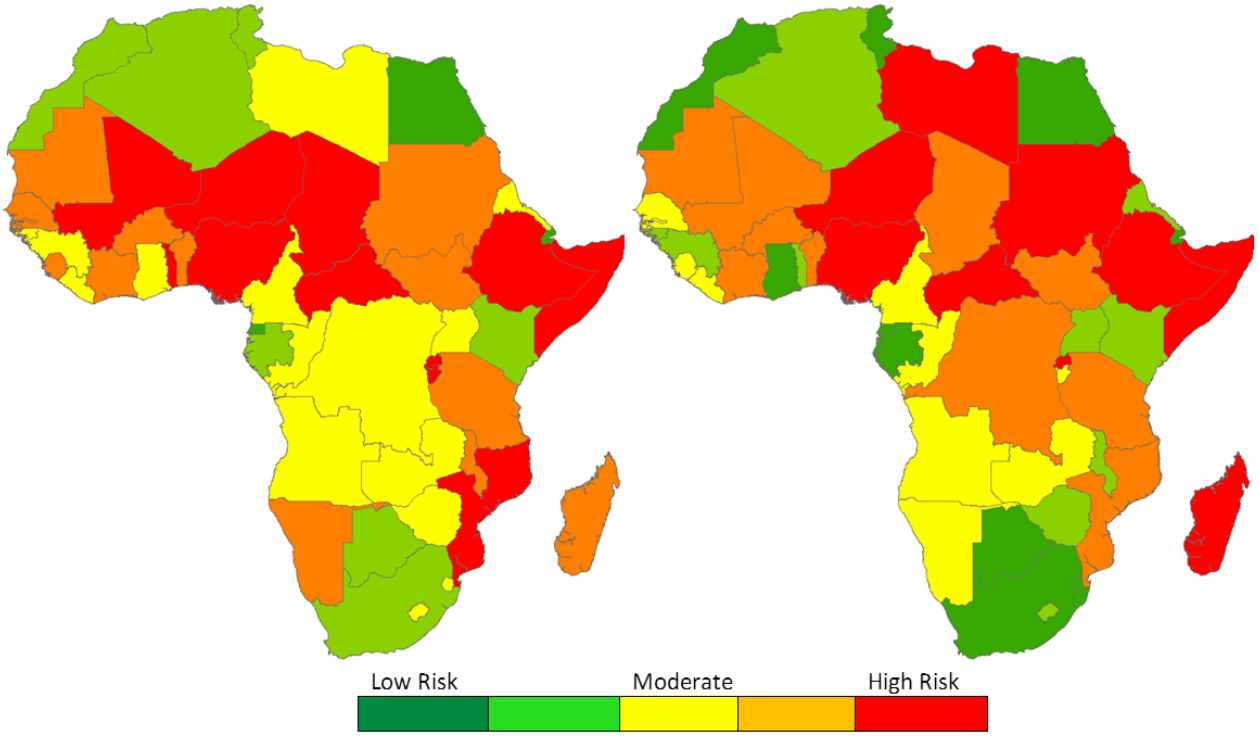

Figure 4-1 Drought risk at country level computed with mean hazard (left) and maximum hazard (right).

In Figure 4-2 are depicted the agricultural risk to droughts using the univariate and bivariate approach to measure the location of the drought prone areas and the DVI calculated by using WWDR-II data (see section 3-2). The main difference between the two methodologies are the higher risk observed in the D.R. of Congo for the univariate method. This difference is mainly due to the period length accounted for each methodology. For the univariate approach, only the last 1980-2010 years where used since the probability under certain threshold have a defined probability of occurrence according with SPI definition if the entire period is used. This period includes the dry period that started in the Congo basin in 1980

and ends in the early 2000's. The bivariate method used the period 1959-2010 which includes both, wet and dry periods in similar proportions.

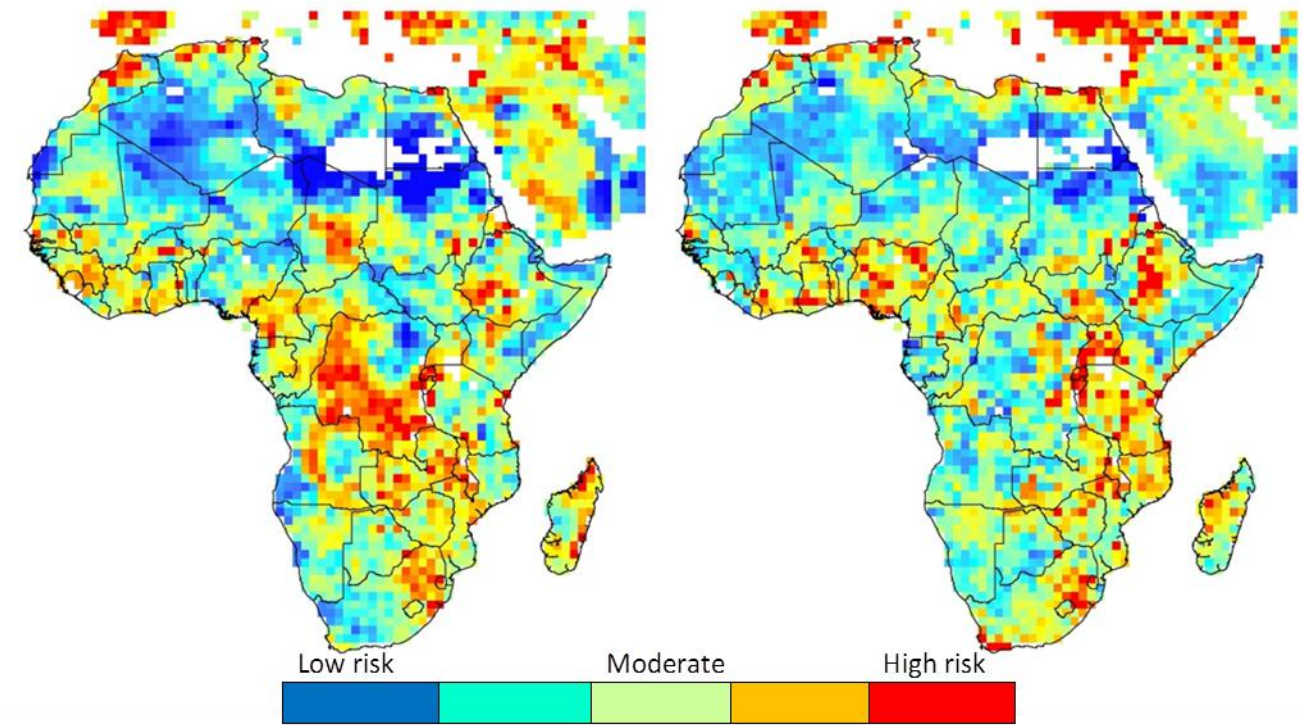

Figure 4-2 Agricultural drought risk using univariate (left) and bivariate (right) approaches.

4.2 RISK ANALYSIS AT SUB BASIN LEVEL

For a regional risk analysis, vulnerability and hazard data was aggregated at sub-basin level. The sub-basin map was determined from the derived HydroSHEDS shapefiles acailable at http://www.worldwildlife.org/hydrosheds. This map was obtained by delineating drainage basin boundaries from hydrologically corrected elevation data with a 15 arc-seconds resolution. The elevation dataset was part of a mapping product, HydroSHEDS, developed by the Conservation Science Program of World Wildlife Fund. Original input data had been obtained during NASA's Shuttle Radar Topography Mission (SRTM).

According to Figure 4-3 the regions most affected by droughts are the Mediterranean coastline of Africa, including the Western Sahara region, the Sahel, the Blue and White Nile sub-basins and the African south eastern coast including the estern part of the Zambezi river, eastern border of the Congo basin and the whole Okavango basin. In this analysis the southern coast of South Africa and northeast of Madagascar are highlighted as well.

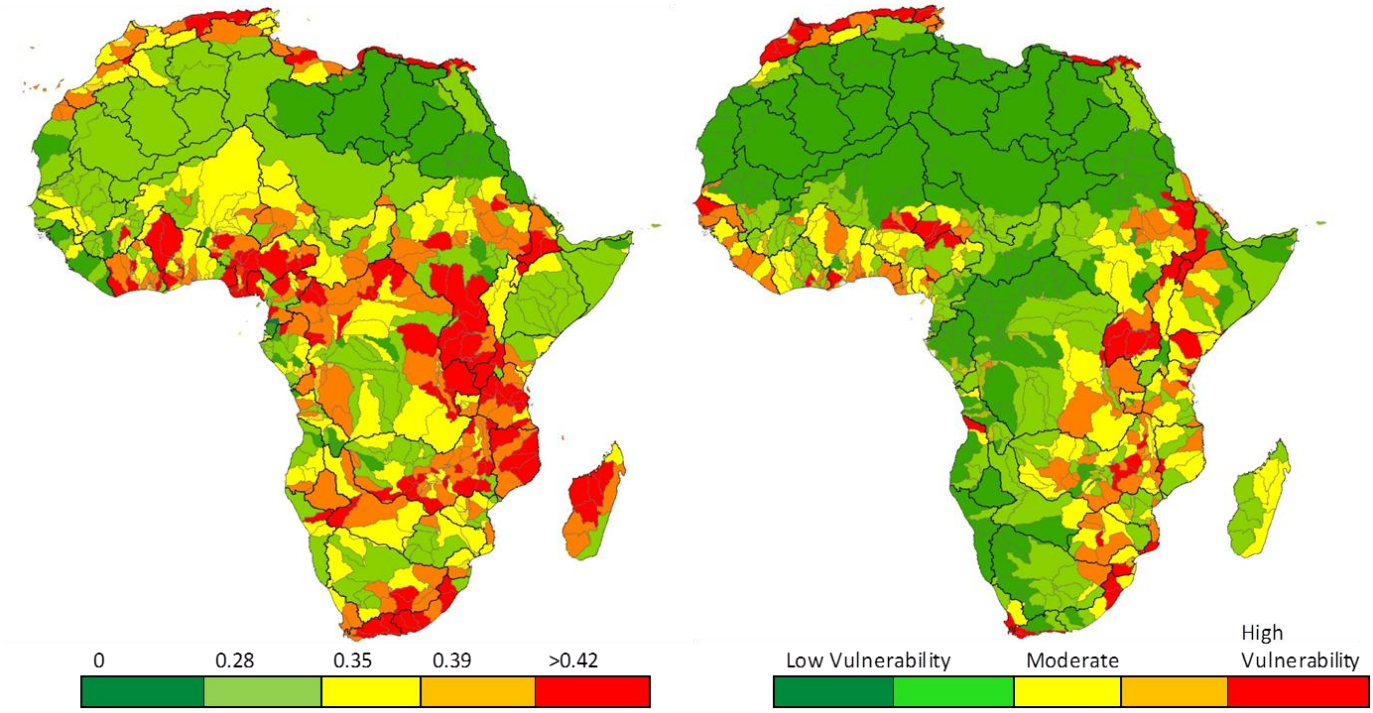

Figure 4-3 Drought hazard (DHI, left) and agricultural vulnerability (right) at sub basin level.

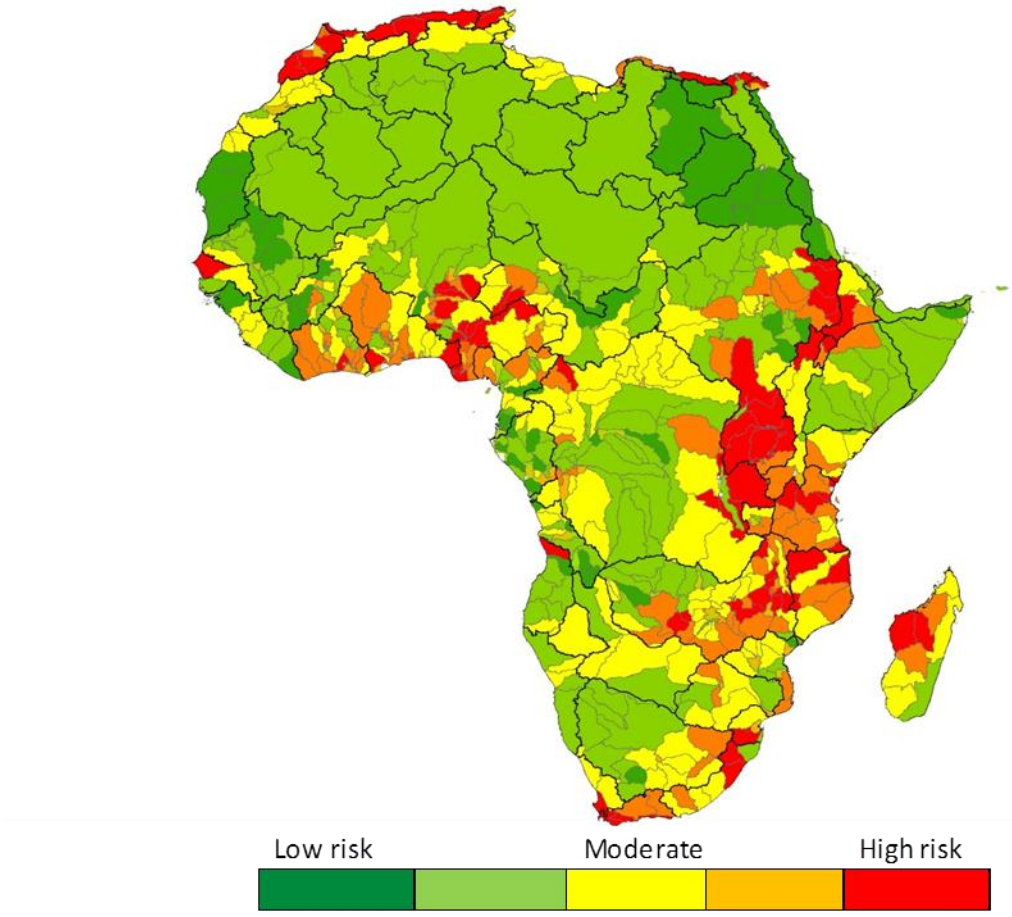

Figure 4-4 Agricultural drought risk at sub basin level.

In the other hand, the regions characterized as more vulnerable (Figure 4 3) show high similarities with the more hazardous regions. The main differences between both risk components were found for Chad and Central African Republic where the agricultural vulnerability tends to be lower compared with other Sahel sub-regions.

Drought risk defined as the product of drought hazard and vulnerability is shown in Figure 4-4. The areas with higher risk (High to moderate in Figure 4-4) can be subdivided in three main different regions. First, the Mediterranean coast of Africa comprising most of the Moroccan (including Oum-er Rbia basin), Algerian basins and the Nile Delta. Secondly, the Sub-Sahara region and the south of Sahel regions with the Volta and Niger and White and Blue Nile.

Thirstly, The Serengeti and the Eastern Miombo woodlands in Tanzania and Mozambique presents high level of drought risk. To these regions should be included the eastern part of the Zambezi river and the Southeastern border of the Congo basin and the belt of Fynbos (natural shrub land vegetation) in the Western Cape of South Africa.

4.3 VALIDATION OF RISK AND VULNERABILITY MAPS

Validate a vulnerability and risk indicator could be extremely difficult. Usually between the most used methods to validate vulnerability and risk indicators are the comparison of those with the impacts of previous drought disasters. This could determine how high levels of vulnerability and/or risk contribute to the impacts of the hazard exposure.

EM-DAT(*) is a global database on natural and technological disasters maintained by the Centre for Research on the Epidemiology of Disasters (CRED) that contains data on the occurrence and effects of natural disasters in the world from 1900 to present. Figure 7-2 shows the number of droughts disasters and the number of persons affected by droughts disasters compiled at the EM-DAT. In a qualitative analysis, it could be seen that countries like Sudan, Ethiopia, Mozambique, Tanzania and Niger reports more than 10.000.000 of persons affected in the period 1970-2006. All those countries are classified as high drought risk according our analysis. Moreover countries that reports more than 1.000.000 of persons affected in this period are classified as moderate to high vulnerability/risk. In this category are Somalia, Mali and Angola among others.

On the other hand, two exceptions to this agreement are Ghana and Kenya where more than 10.000.000 of persons have been reported during the 1970-2006 period but are classified as low risk. Thais disagreement could be because the aggregation of the hazard from pixel to national level, since both countries are classified as moderate to high risk in the pixel and sub-basin level analysis (see Figure 4-2 and Figure 4-4).

in order to asses how the risk and vulnerability indicators are correlated with drought disasters the tetrachoric correlation (Drasgow, 1986) was computed between the number of persons affected (PRA) and the different components of the drought risk (i.e. Hazard and Vulnerability indicators). The variables were converted to dichotomous variables by splitting the scale at the median and designating individuals above and below that point as defining two separate groups. After the dichotomization, the variables are treated as a categorical variable and a tetrachoric test was carried out to determine whether there is a significant difference in the groups represented by the dichotomized variables.

Table 4-1 shows the contingency tables and tetrachoric coefficients for the dichotomized number of PRA with the DVI and drought risk computed with mean DHI. This result shows a significative (with a 95% confidence interval) direct relation between the impacts and the indicators. For the drought risk computed with the maximum value of DHI for each country a positive relation is observed but the results are not significative. However in both cases the amount of information is not enough to display conclusive results.

(A)	Low DVI	High DVI
Low Nº PRA	16	7
High Nº PRA	7	17
r_t =0.593 σ_{rt}=0.1688		
(B)	Low Risk	High Risk
Low Nº PRA	14	7
High Nº PRA	7	15
r_t =0.521 σ_{rt}=0.192		

Table 4-1 Contingency tables and tetrachoric coefficient (r_t) for (A) Number of persons reported affected (PRA) by droughts disasters and DVI and (B) Number of persons reported affected by droughts disasters and Drought risk computed with average hazard.

(*)EM-DAT: The OFDA/CRED International Disaster Database – www.emdat.be, Université Catholique de Louvain, Brussels (Belgium).

5. CONCLUSIONS

This research combines drought hazard maps computed with two different approaches with a drought vulnerability index in order to evaluate the drought risk. This risk analysis was performed both, at regional (pixel and sub-basin) and country level.

According with the hazard characterization the main desert areas characterized by a hot and arid climate (Sahara and Kalahari) are associated with low values of drought hazard. Included in this category are also the Tropical moist deciduous forest zones in Central Africa (mainly in Angola, Zambia and South D.R of Congo) where the region is characterized by an overall low probability of drought occurrence.

On the other hand, the more drought prone areas are the Mediterranean coast of Africa (associated with a markedly dry summer), the equatorial regions with a dry winter, the Sahel, southern east Africa, and the wet part of southern South Africa.

A drought vulnerability index was constructed using socio-economic data at country level. This indicator is able to represent the complex processes that could lead to social drought vulnerability. However, it must be used critically taking into account that their construction relies on some level of subjectivity and theoretical assumptions. According to this analysis, the countries classified with higher relative vulnerability are Somalia, Mali, Ethiopia, Niger, Burundi and Chad.

Risk is defined as the combination of capacity of a society to cope, resist and recover from any certain impact (vulnerability) and the drought hazard that threat the social system. In general, the countries and regions whit highest levels of drought risk tend to be those that are more vulnerable, this means that vulnerability are a determinant factor independently of the hazard. At country level Sudan, Ethiopia, Mozambique, Tanzania, Chad, Nigeria and Mali belong to the moderate high to high risk classes, while Botswana, South Africa, Gabon, Morocco, Tunisia and Egypt are characterized as low risk.

A regional analysis shows that the basins with high to moderate drought risk can be subdivided in three main different geographical regions: the Mediterranean coast of Africa (comprising most of the Moroccan and Algerian basins and the Nile Delta); the Sub-Sahara and the south of Sahel regions (including the Volta, Niger, White and Blue Nile); the Serengeti and the Eastern Miombo woodlands of Tanzania and Mozambique. Additionally, the eastern part of the Zambezi basin, the South-eastern border of the Congo basin and the belt of Fynbos in the Western Cape should also be included in this category.

Even if the results are not conclusive, a good agreement is observed between the drought vulnerability and risk maps and the number of persons affected by droughts. There is a need to validate the vulnerability indicator with appropriate disaster data in order to measure and improve the robustness of the indicator and explain why in some cases extreme droughts can lead to disasters while in other cases their impact is much lower.

6. REFERENCES

AghaKouchak A., D. Easterling, K. Hsu, S. Schubert, S. Sorooshian, 2013. Extremes in a Changing Climate: Detection, Analysis and Uncertainty. Springer, 437 p.

Ailliot, P. and Thompson, C.; 2011; Mixed methods for fitting the GEV distribution; Water Resources Research, Vol 47

Berg D., 2009. Copula Goodness-of-Git Testing: An Overview and Power Comparison. The European Journal of Finance, 15, 675-701.

Birkmann J, 2007: Risk and vulnerability indicators at different scales: applicability, usefulness and policy implications. Environ Hazards 7:20–31

Bohle H.-G. 2001. Vulnerability and Criticality: Perspectives from Social Geography, IHDP Update 2/2001, Newsletter of the International Human Dimensions Programme on Global Environmental Change, 1–7.

Bonett, D. G., Price R. M. 2005: Inferential Methods for the Tetrachoric Correlation Coefficient. Journal of Educational and Behavioral Statistics, 30, 213-225.

Brooks, N., 2003. Vulnerability, Risk and Adaptation: A Conceptual Framework. Working Paper 38, Tyndall Centre for Climate Change Research, University of East Anglia, Norwich.

Cherubini U, Luciano E, Vecchiato W 2004: Copula Methods in Finance. John Wiley & Sons.

Clayton DG 1978. “A Model for Association in Bivariate Life Tables and Its Application in Epidemiological Studies of Familial Tendency in Chronic Disease Incidence.” Biometrika, 65, 141–152.

Coles,S. and Davison, A.; 2008: Statistical Modelling of Extreme Values; Based on ‘An Introduction to Statistical Modeling of Extreme Values’,by Stuart Coles, Springer, 2001.

Conway, Declan, Aurelie Persechino, Sandra Ardoin-Bardin, Hamisai Hamandawana, Claudine Dieulin, Gil Mahé, 2009. Rainfall and Water Resources Variability in Sub-Saharan Africa during the Twentieth Century. J. Hydrometeor, 10, 41–59

De Michele, C. and Salvadori, G. 2003. A Generalized Pareto intensity-duration model of storm rainfall exploiting 2-Copulas. Journal of Geophysical Research 108.

DEWFORA D2.2, 2011: Inventory of institutional frameworks and drought mitigation and adaptation practices in Africa. http://www.dewfora.net/Publications

DEWFORA D3.2, 2012. Methods for mapping drought vulnerability at different spatial scales. http://www.dewfora.net/Publications

DEWFORA D6.3, 2012. Testing of drought indicators at Pan-African level. http://www.dewfora.net/Publications

Drasgow, F. 1986: Polychoric and polyserial correlations. Pp. 68–74 in S. Kotz and N. Johnson, eds., The Encyclopedia of Statistics, Volume 7. Wiley.

FAO 2000: Global Forest Resources Assessment. www.fao.org/forestry/fo/fra/index.jsp (FRA subject page) and www.fao.org/forestry/fo/country/nav_world.jsp (FAO Forestry country profiles).

Fermanian JD, 2005: Goodness of fit tests for copulas , J. Multivariate Anal, 95, 119-152.

Frank MJ, 1979. On the Simultaneous Associativity of F(x, y) and x + y − F(x, y). Aequationes Mathematicae, 19, 194–226.

Frees EW, Valdez EA 1998: Understanding Relationships Using Copulas. North American Actuarial Journal, 2(1), 1–25.

Frees EW, Wang P, 2005: Credibility Using Copulas. North American Actuarial Journal, 9(2), 31–48.

Genest C, Favre AC 2007. Everything you always wanted to know about copula modeling but were afraid to ask. J Hydrol Eng 12 (4):347–368.

Genest, C. and Remillard, B. 2008. Validity of the parametric bootstrap for goodnessof-fit testing in semiparametric models. Ann. Inst. H. Poincare Probab. Statist. 44 1096–1127.

Genest C., B. Rémillard, D. Beaudoin, 2009. Goodness-of-fit tests for copulas: A review and a power study, Insurance: Mathematics and Economics, 44, 199-213.

Green, Reginald Herbold. 1993. The Political Economy of Drought in Southern Africa. Health Policy and Planning 8, No. 3: 255-266.

Gumbel EJ 1960. Bivariate Exponential Distributions. Journal of the American Statistical Association, 55, 698–707.

Hofert M., M. Maechler 2011. Nested Archimedean Copulas Meet R: The nacopula Package. Journal of Statistical Software, 39(9), 1-20. URL http://www.jstatsoft.org/v39/i09/.

Hulme M 1996. Climatic change within the period of meteorological records. In: Adams WM, Goudie AS, Orme AR (eds) The physical geography of Africa. Oxford University Press, Oxford, p 88–102.

Husak, G. J., Michaelsen, J. and Funk, C. 2007: Use of the gamma distribution to represent monthly rainfall in Africa for drought monitoring applications. International Journal of Climatology, 27: 935–944. doi: 10.1002/joc.1441

Iglesias A, Garrote L, Cancelliere A, Cubillo F, and Wilhite D, 2009: Coping with Drought Risk in Agriculture and Water Supply Systems. Springer.

ILRI; 2006; Mapping climate vulnerability and poverty in Africa; The International Livestock Research Institute (ILRI), Kenya.

Joe H, 1997. Multivariate Models and Dependence Concepts. Chapman & Hall Ltd.

Kane, R.P. 2009. Periodicities, ENSO effects and trends of some South African rainfall series: an update. S. Afr. j. sci., 105, pp. 199-207

Kao, S.C. and R. S. Govindaraju 2008: Trivariate Statistical Analysis of Extreme Rainfall Events via Plackett Family of Copulas, Water Resources Research, 44.

Kojadinovic I, Yan J, 2010. Modeling Multivariate Distributions with Continuous Margins Using the copula R Package. Journal of Statistical Software, 34(9), 1-20. URL http://www.jstatsoft.org/v34/i09/.

Kruger A.C. 2006. Observed trends in daily precipitation indices in South Africa: 1910–2004. Int. J. Climatol. doi:10.1002/joc.1368

Laraque A., G. Mahé, D. Orande, B. Marieu, 2001. Spatiotemporal variations in hydrological regimes within Central Africa during the XXth century. Journal of Hydrology, 245, 104–107

Lee, T., and J. D. Salas, 2011: Copula-based stochastic simulation of hydrological data applied to Nile River flows, Hydrol. Res., 42(4), 318–330.

Lee T, Modarres R, Ouarda T, 2012: Data-based analysis of bivariate copula tail dependence for drought duration and severity. Hydrol. Processes. Doi: 10. 1002/hyp. 9233.

Lloyd-Hughes, B., and M. A. Saunders, 2002: A drought climatology for Europe. Int. J. Climatol., 22, 1571–1592.

McKee T.B., Doesken N.J., Kleist J., 1993: The Relationship of Drought Frequency and Duration to Time Scales. Proc. 8th Conf. on Appl. Clim., 17-22 Jan. 1993, Anaheim, CA, 179-184.

McKee, T. B., N. J. Doesken, and J. Kleist, 1995: Drought monitoring with multiple time scales. Proc. Ninth Conf. on Applied Climatology, Dallas, TX, Amer. Meteor. Soc. 233-236.

Moron, V. 1997. Trend, decadal and interannual variability in annual rainfall of subequatorial and tropical North Africa (1900–1994). Int. J. Climatol., 17: 785–805

Mutua, F. M. and Zaki, A.F.; 2010; Analyses of Annual Droughts in Kenya Using an Objective Annual Rainfall Drought Index; J.Meteorol. Rel. Sci., Vol 4, pp. 21–33

Naumann G., P. Barbosa, H. Carrao, A. Singleton, and J. Vogt, 2012: Monitoring drought conditions and their uncertainties in Africa using TRMM data. J. of Applied Meteorology and Climatology, 51, 1867–1874.

Nelsen RB 2006. An introduction to copulas. Springer, New York

Nicholson SE, Entekhabi D, 1986. The quasi-periodic behavior of rainfall variability in Africa and its relationship to the Southern Oscillation. Arch Meteorol Geophys Bioclimatol Ser A 34:311–348

Nicholson SE, 1994. Recent rainfall fluctuations in Africa and their relationships to past conditions over the continent. The Holocene 4:121–131

Nicholson SE, 2000. A semi-quantitative, regional precipitation data set for studying African climates of the nineteenth century, Part I. Overview of the data set. Climate Change.

Nicholson, S.E. 2001: Climatic and environmental change in Africa during the last two centuries. Climate Research 17: 123-144.

United Nations, 1991: Mitigating Natural Disasters: Phenomena, Effects, and Options: a Manual for Policy Makers and Planners, New York: UNDRO (United Nations Disaster Relief Organization).

United Nations Development Programme (UNDP), 2004: Reducing Disaster Risk – A challenge for development – A Global Report, ISBN 92-1-126160-0, New York, USA.

Salvadori, G., and C. De Michele 2004: Analytical calculation of storm volume statistics with Pareto-like intensity-duration marginals, Geophys. Res. Lett., 31, L04502.

Schweizer, B. and Sklar, A., 1983, Probabilistic Metric Spaces, Elsevier Science Publishing Co., New York.

Sklar A 1959. Fonctions de répartition à n dimensions et leurs marges. Publ Inst Statist Univ Paris 8:229–231

Shiau JT. 2006. Fitting drought duration and severity withtwo-dimensional copulas. Water Resources Management 20:795–815.

Shiau JT, Feng S, Nadarajah S. 2007. Assessment of hydrologicaldroughts for the Yellow River, China using copulas. HydrologicalProcesses 21:2157–2163

Shiau J, Hsiao Y, 2012: Water-deficit-based drought risk assessments in Taiwan. Nat Hazards, 64:237–257

Thom H.C., 1958: A note on the gamma distribution. Monthly Weather Review 86: 117–122.

Vörösmarty, C.J., P. Green, J. Salisbury, and R. Lammers. 2000. Global water resources: Vulnerability from climate change and population growth. Science 289: 284-288.

Vörösmarty, C.J., E.M. Douglas, P.A. Green, and C. Revenga. 2005. Geospatial indicators of emerging water stress: An application to Africa. Ambio. 2005 May;34(3):230-6.

Wilhite, D. A. and Svoboda, M. D., 2000, 'Drought early warning systems in the context of drought preparedness and mitigation', in Early Warning Systems for Drought Preparedness and Drought Management, World Meteorological Organization, Lisboa, 1–21.

Wilks D.S. 2002: Statistical Methods in the Atmospheric Sciences. Elsevier Academic Press Publications: pp. 467.

Yan J., 2007. Enjoy the Joy of Copulas: With a Package copula. Journal of Statistical Software, 21(4), 1-21. URL http://www.jstatsoft.org/v21/i04/.

7. APPENDICES

7.1 APPENDIX A

The copulas analysis was performed using the R package Copula (Yan 2007; Kojadinovic and Yan 2010; Hofert and Maechel 2011). Two most frequently used copula families are elliptical copulas and Archimedean copulas. An elliptical copula is the copula corresponding to an elliptical distribution by the Sklar's theorem. Let F be the multivariate CDF of an elliptical distribution and Fi the CDF of the i^{th} margin and F_i^{-1} be its inverse function for i=1,...,p. Then the elliptical copula determined by F is

$$\boldsymbol{C(u_1, \dots, u_p) = F[F_1^{-1}(u_1), \dots, F_p^{-1}(u_p)]} \quad \textbf{7–1}$$

Elliptical copulas are widely used in finance and risk management because of their easy implementation. Convenience in obtaining conditional distributions is another advantage in using them for predicting (Frees and Wang 2005). In this work, the normal elliptical copula was tested.

Archimedean copulas are constructed through a generator φ defined as

$$\boldsymbol{C(u_1, \dots, u_p) = \varphi^{-1}\{\varphi(u_1), \dots, \varphi(u_p)\}} \quad \textbf{7–2}$$

where φ^{-1} is the inverse of the generator φ. In order for C to be a copula, the generator needs to be a p-monotonic function (Nelsen, 2006). A generator uniquely (up to a scalar multiple) determines an Archimedean copula. Details of generators for various Archimedean copulas can be found in Nelsen (2006). In this study three Archimedean copula classes were tested: the Clayton copula (Clayton, 1978), Frank copula (Frank, 1979) and Gumbel copula (Gumbel, 1960).

For an elliptical copula the evaluation of its distribution requires the fitting of the joint CDF of the elliptical distribution and univariate quantile function for each marginal distribution. By differentiating the density of an elliptical copula are obtained;

$$\boldsymbol{C(u_1, \dots, u_p) = \frac{f[F_1^{-1}(u_1), \dots, F_p^{-1}(u_p)]}{\prod_{i=1}^{p} f_i[F_i^{-1}(u_i)]}} \quad \textbf{7–3}$$

Where f is the joint PDF of the elliptical distribution and $f_1,\dots,f_p$ are the marginal density functions.

For an Archimedean copula, the distribution and density depends on the generator function and its inverse function.

The five, empirical, elliptical and Archimedean copulas used in this study are listed below:

Empirical Copula: Let $\{(R_k,S_k)\}$ be the ranks associated with the sample $\{(X_k,Y_k)\}$, k=1,…,n. The corresponding empirical copula (Genest and Favre, 2007) C_n is defined as:

$$\mathbf{C}_{\boldsymbol{n}}(\boldsymbol{u},\boldsymbol{v}) = \frac{\mathbf{1}}{\boldsymbol{n}}\sum_{\boldsymbol{k}=\mathbf{1}}^{\boldsymbol{n}} \mathbf{1}\left(\frac{\boldsymbol{R_k}}{\boldsymbol{n}+\mathbf{1}} \leq \boldsymbol{u}, \frac{\boldsymbol{S_k}}{\boldsymbol{n}+\mathbf{1}} \leq \mathbf{v}\right) \qquad \textbf{7–4}$$

Where u,v I and 1 is an indicator function. As the univariate case, the empirical copula counts the number of pairs that satisfy the given conditions. The main advantage is that the construction of this copula is non-parametric, since only the ranks of the data are needed (AghaKouchak et al, 2013).

Normal Copula: For a given correlation matrix $\Sigma \in \Re^{dxd}$, the Gaussian copula with parameter matrix Σ can be written as

$$\boldsymbol{C}(\boldsymbol{u},\boldsymbol{v}) = \boldsymbol{\Phi_\theta}\left(\boldsymbol{\Phi}^{-\mathbf{1}}(\boldsymbol{u}), \boldsymbol{\Phi}^{-\mathbf{1}}(\boldsymbol{v})\right), -\mathbf{1} \leq \boldsymbol{\theta} \leq \mathbf{1} \qquad \textbf{7–5}$$

where Φ^{-1} is the inverse cumulative distribution function of a standard normal and Φ_Σ is the joint cumulative distribution function of a multivariate normal distribution with mean vector zero and covariance matrix equal to the correlation matrix Σ.

The density can be written as

$$\boldsymbol{C_N}(\boldsymbol{u},\boldsymbol{v};\boldsymbol{\Sigma}) = \int_{-\infty}^{\boldsymbol{\Phi}^{-\mathbf{1}}(\boldsymbol{u_1})} \int_{-\infty}^{\boldsymbol{\Phi}^{-\mathbf{1}}(\boldsymbol{v})} \frac{\mathbf{1}}{\sqrt{(\mathbf{2}\boldsymbol{\pi})^{\boldsymbol{n}}|\boldsymbol{\Sigma}|}} \boldsymbol{e}^{-\frac{\mathbf{1}}{\mathbf{2}}\boldsymbol{x}\boldsymbol{\Sigma}^{-\mathbf{1}}\boldsymbol{x}}\boldsymbol{dx} \qquad \textbf{7–6}$$

Gumbel Copula:

$$\boldsymbol{C}(\boldsymbol{u},\boldsymbol{v}) = \boldsymbol{e}^{\{-[(-\boldsymbol{lnu})^{\boldsymbol{\theta}}+((-\boldsymbol{lnv})^{\boldsymbol{\theta}})]\}} \qquad \textbf{7–7}$$

Where θ are the dependence parameter that represents the degree of association between u and v.

Frank Copula:

$$\boldsymbol{C}(\boldsymbol{u},\boldsymbol{v}) = -\frac{\mathbf{1}}{\boldsymbol{\theta}}\mathbf{ln}\left[\mathbf{1} + \frac{(\boldsymbol{e}^{-\boldsymbol{\theta u}}-\mathbf{1})|\boldsymbol{e}^{-\boldsymbol{\theta v}}-\mathbf{1}|}{\boldsymbol{e}^{-\boldsymbol{\theta}}-\mathbf{1}}\right], \ \boldsymbol{\theta} \neq \mathbf{0} \qquad \textbf{7–8}$$

Clayton Copula:

$$\boldsymbol{C}(\boldsymbol{u},\boldsymbol{v}) = (\boldsymbol{u}^{-\boldsymbol{\theta}} + \boldsymbol{v}^{-\boldsymbol{\theta}} - \mathbf{1})^{\frac{-\mathbf{1}}{\boldsymbol{\theta}}}, \ \boldsymbol{\theta} > \mathbf{0} \qquad \textbf{7–9}$$

The goodness of fit of each copula was tested using the nonparametric empirical copula to compare with the theoretical copulas. The parametric copula that was closest to the empirical copula was defined as the most appropriate choice (Genest and Favre 2007).

Empirical copulas are rank-based, empirically joint cumulative probability measures (Nelsen 2006). For the bivariate case, the empirical copula of the observed data is described by Equation 7-4. One measure of fit is based on how close the points of each copula are to the diagonal line ($d_i=s_i$).

As the empirical copula is the observed frequency of $P(Z_1 < u_1, Z_2 < u_2)$, it is feasible to compare C(z) with a parametric estimation of $C_\theta(z)$. This is a very natural approach for copula Goodness-of-Fitting testing considering that most univariate g-o-f tests are based on a distance between empirical and null hypothesis distribution functions. Genest et al. (2009) state that, given that it is entirely non-parametric, C(z) is the most objective benchmark for testing the copula g-o-f. The statistic approach following Genest et al., 2009 is:

$$\boldsymbol{S_n = n \int_{[0,1]^d} \{C(z) - C_\theta(z)\}^2 dC(z) = \sum_{j=1}^{n} \{C(z_j) - C_\theta(z_j)\}^2} \quad \textbf{7–10}$$

and

$$\boldsymbol{T_n = sup\left|\sqrt{n}(C(z) - C\theta(z))\right|} \quad \textbf{7–11}$$

In Fermanian (2005) was stated that this methodology seem to be unpractical, except by bootstrapping. The implementation of a bootstrap approach is depicted in Genest and Rémillard (2008), where a rank-based version of the familiar Cramér–von Mises and Kolmogorov–Smirnov were applied.

Large values of these statistics (S_n and T_n) lead to the rejection of H_0 (H_0: $C \in C_0$, Therefore, the goodness-of-fit consist in comparing a "distance" between C(z) and an estimation $C_\theta(z)$ of C obtained under H_0). Approximate P-values can be deduced from their limiting distributions, which depend on the asymptotic behavior of the process C_n. Genest and Rémillard (2008) show that the tests based on S_n and T_n are consistent; i.e., if $C \notin C_0$, then H_0 is rejected with probability 1 as $n \to \infty$.

	Parameter (θ)	S_n	p
Gumbel	4.25	0.0790	0.000499
Frank	**18.71**	**0.0598**	**0.000499**
Normal	0.95	0.0659	0.00148
Clayton	5.43	0.0936	0.001498

Table 7-1 Goodness-of-fit tests for the different copulas based on the empirical process (comparing the empirical copula with a parametric estimate of the copula derived under the null hypothesis) in one pixel in the Limpopo Basin. The test statistic is the Cramer-von Mises functional S_n (Equation 7-11) and approximate p-values for the test statistic obtained using parametric bootstrap. In bold are indicated the best performance.

As an example, Table 7-1 shows the comparative S_n for the different copula functions used in this study. A lower S_n value implies a better fit (lowest distance between the empirical and the parametric copulas). In this case, the Frank copula shows the better performance with the lowest value of S_n.

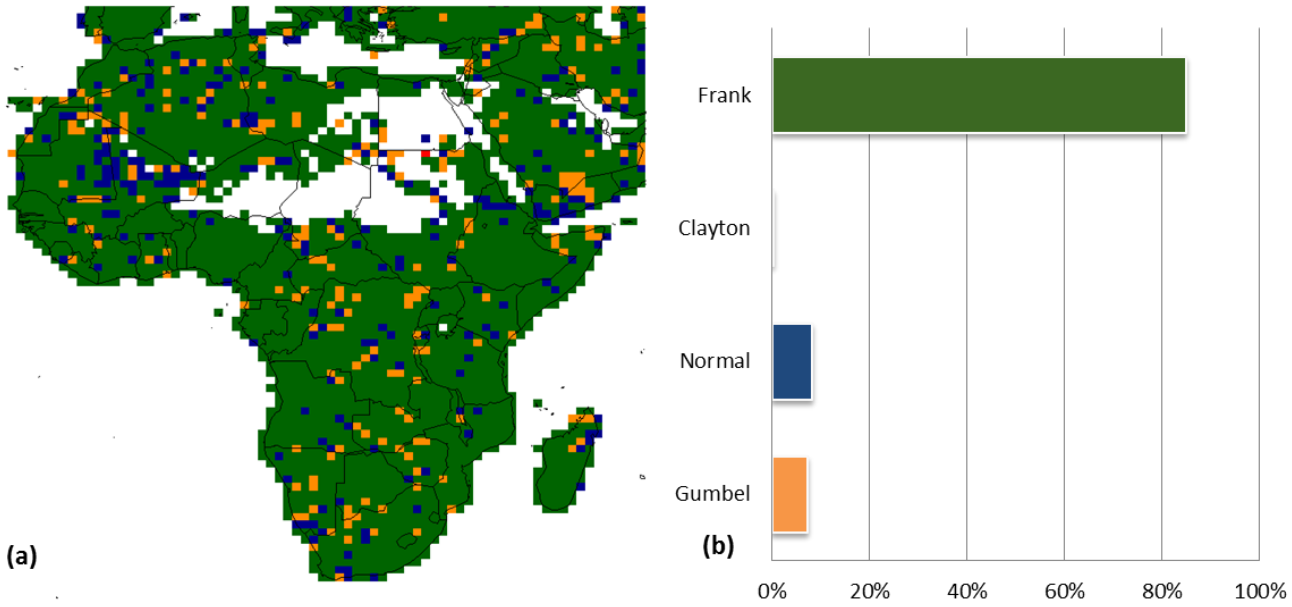

Figure 7-1 (a) Map Copula functions with the best performance and (b) percentage of pixels where each copula shows the best performance.

Figure 7-1 shows the membership of each pixel to the best fit copula according with Equation 7-11. At continental scale The Frank copula is the best function with 84% of the pixels having the lowest S_n. Normal and Gumbel functions represents 8% and 7% of total pixels respectively, while Clayton copula best perform in only one pixel.

7.2 APPENDIX B

Author(s)	Risk definition
Smith, 1996 (p5)	Probability x loss (probability of a specific hazard occurrence) *Hazard = potential threat*
IPCC, 2001 (p21)	Function of probability and magnitude of different impacts
Morgan and Henrion, 1990 (p1)/Random House, 1966	"Risk involves an 'exposure to a chance injury or loss'"
Adams, 1995 (p8)	"a compound measure combining the probability and magnitude of an adverse affect"
Jones and Boer, 2003; (also Helm, 1996)	Probability x consequence *Hazard: an event with the potential to cause harm, e.g. tropical cyclones, droughts, floods, or conditions leading to an outbreak of disease-causing organisms.*
Downing et al., 2001	Expected losses (of lives, persons injured, property damaged, and economic activity disrupted) due to a particular hazard for a given area and reference period *Hazard: a threatening event, or the probability of occurrence of a potentially damaging phenomenon within a given time period and area.*
Downing et al., 2001	Probability of hazard occurrence *Hazard = potential threat to humans and their welfare*
Crichton, 1999	"Risk" is the probability of a loss, and depends on three elements, hazard, vulnerability and exposure."
Stenchion, 1997	"Risk might be defined simply as the probability of occurrence of an undesired event [but might] be better described as the probability of a hazard contributing to a potential disaster…importantly, it involves consideration of vulnerability to the hazard."
UNDHA, 1992	"Expected losses (of lives, persons injured, property damaged, and economic activity disrupted) due to a particular hazard for a given area and reference period. Based on mathematical calculations, risk is the product of hazard and vulnerability."

Table 7-2 Different approaches to risk and hazard definition. Source: Brooks, 2003

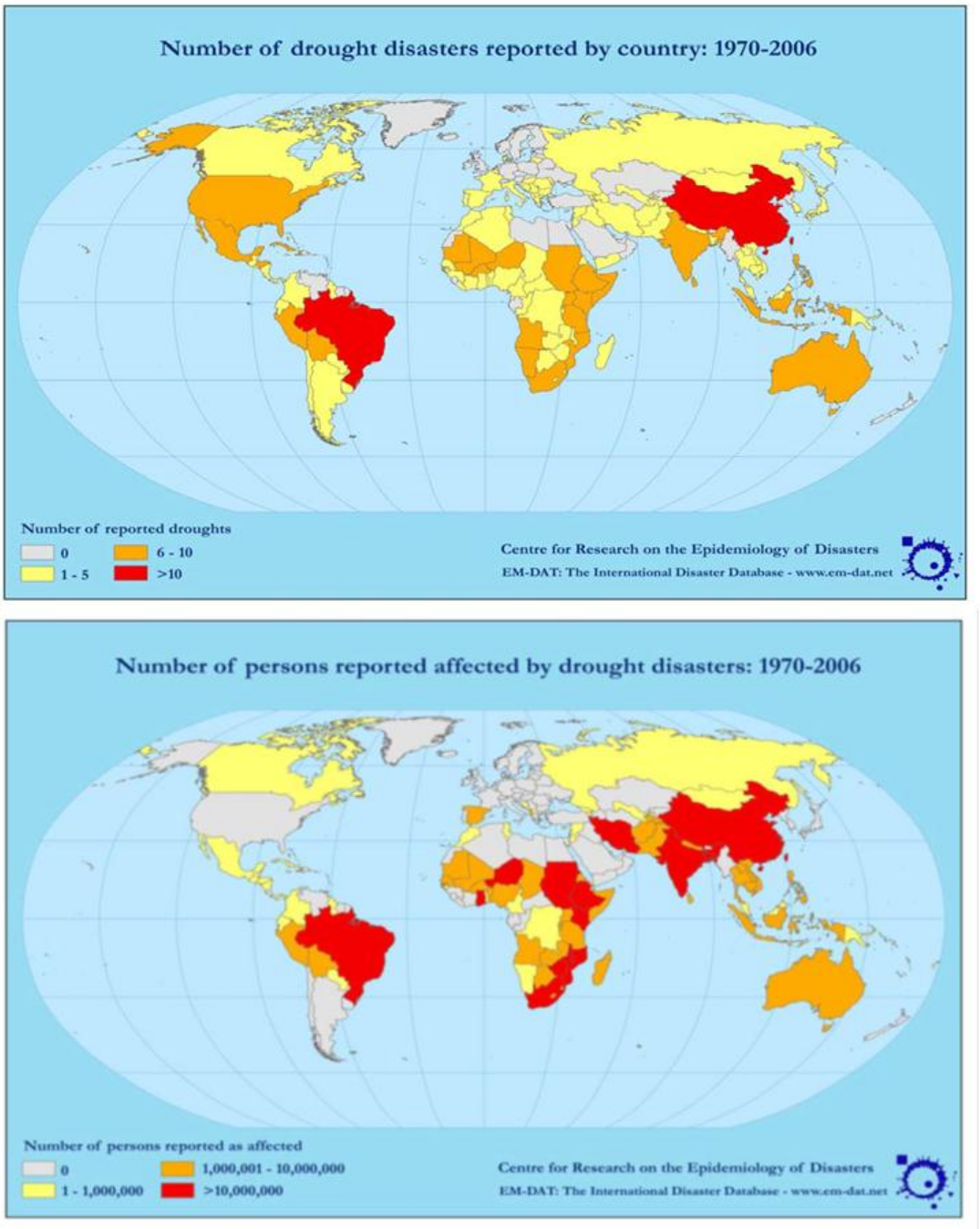

Figure 7-2 Number of drought disasters (top) and persons affected by droughts disasters (bottom). Source: CRED CRUNCH newsletter, December 2006, Centre for Research on the Epidemiology of Disasters, Brussels, Belgium;

http://www.em-dat.net/documents/CRED%20CRUNCH%207%20-%20December%202006.pdf

7.3 APPENDIX C

Indicators	Total water use	GDP per capita US$	Energy use	Population living below $1.25 PPP per day	Institutional capacity	Adult literacy rate	Population without improved water	Fertilizer consumption	Water infrastructure
Algeria				1					
Benin				1					
Botswana				1				C	
Burkina F.			C	1					
Burundi			C						
Cape Verde			C	1	1			C	
C. A. R.			C					C	
Chad				1				C	
Comoros				1	1			C	
Congo D. R.						1			
Djibouti				1		1		1	
Eq. Guinea				1				1	
Eritrea				1					
Gambia				1					
Guinea			C						
Guinea B.				1				C	
Lesotho				1				C	
Liberia			C					1	
Libya				1			1		
Madagascar			C						
Malawi			C	1					
Mali			C						
Mauritania			C					C	
Mauritius				1					
Namibia				1					
Niger			C						
Nigeria				1					
Rwanda			C						
S. Tome P.	1			1				1	
Seychelles	1								1
S. Leone			C	1				C	
Somalia		C	C	1				C	
Sudan (*)				1					
Swaziland				1				C	

Indicators	Total water use	GDP per capita US$	Energy use	Population living below $1.25 PPP per day	Institutional capacity	Adult literacy rate	Population without improved water	Fertilizer consumption	Water infrastructure
Uganda			C						
Zambia				1					
Zimbabwe		C		1					
Total	2	0	0	25	2	2	1	4	1
% missing data	3.7	0.0	0.0	46.3	3.7	3.7	1.9	7.4	1.9

Table 7-3 Details of missing data for each indicator and country. Only countries and indicators that present missing values are showed. Indicators flagged with C represent missing data completed with different sources. **(*) Sudan and South Sudan**

7.4 APPENDIX D: REGIONAL VULNERABILIY AND RISK ANALYSIS IN KENYA

7.4.1 Drought frequency analysis

The study utilized monthly rainfall data for the period 1961 to 2011 for sixteen stations located in Kenya. The distribution of the stations used is shown in Figure 7-3; these stations were selected due to availability of complete monthly data for the period.

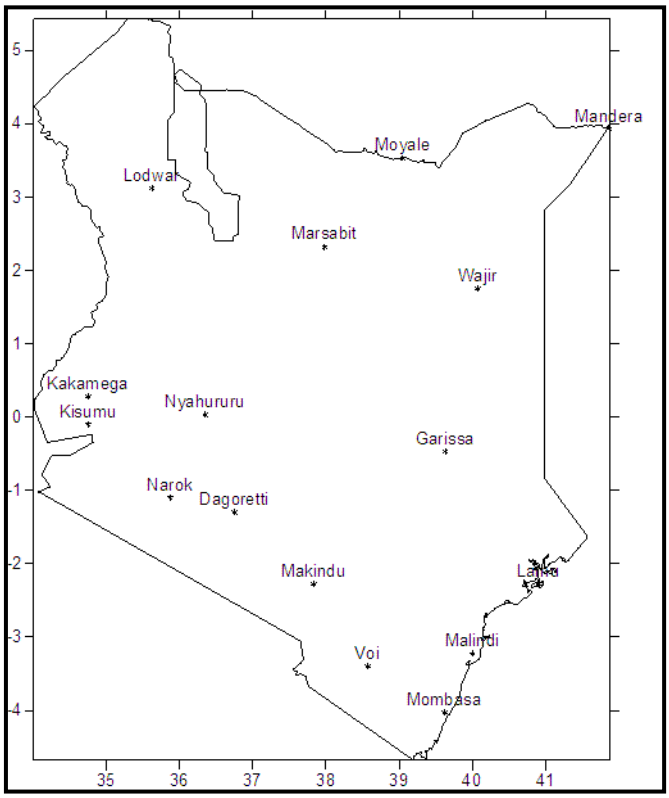

Figure 7-3 Spatial distribution of stations used.

To study the drought frequency, an annual drought index was tested. The index proposed was first developed by Mutua and Zaki (2010) on the basis of the understanding that socio-economic factors notwithstanding, the aggregated annual rainfall deficit is crucial in defining the level of intensity of the annual drought. The deficits require the determination of a monthly threshold for establishing the level of the monthly rainfall deficit. It is also recognized that while the total number of rainfall deficit-months is important in determining the annual drought intensity, it is the maximum run-length of the deficit-months that truly amplifies the annual drought. They adopted a monthly threshold given by the 55-percentile of the annual monthly rainfall.

The annual drought index was defined as a power function of the absolute sum of the normalized rainfall deficit which fall below the threshold for every month of the year. The annual value of the power factor is given by the largest relative run-length of the deficit-

months in a given year, while the multiplier coefficient in the power function is given by the fraction of the deficit-months in the year. Mathematically, the annual drought index D_i for year i, is expressed as:

$$\boldsymbol{D_i = A_i \left[\sum_{i=1}^{n} \left|Z_{i,j}\right|\right]^{B_i}} \quad 7.4.1$$

Where, n represents the data length in years, the subscript j denoted the month of year i and $|Z_{i,j}|$ is the magnitude of the rainfall deficit in the month j of year i, which is defined as:

$$\boldsymbol{Z_i = \left\{\frac{X_{i,j} - P_j^{55\%}}{\sigma_j}\right.} \quad 7.4.2$$

Where,

$Z_{i,j}$= the rainfall in month j of year i in the given station.
$P^{55\%}$ = the annual monthly 55-percentile of the rainfall which has an annual monthly standard deviations S_j for the given month j in year i.
A_i = the fraction of the deficit-months in year i, and
B_i = the largest relative run-length of the deficit-months in year i

The drought indices generated by equation (7.4.1) above formed the basis for further analysis. The initial step was to compare these indices with the actual annual rainfall for the 16 stations; results from two stations are discussed below.

Figures 7-4 and 7-5 show the distribution of the annual drought index in comparison to the distribution of the annual rainfall in two rainfall stations from the study cases. Figures 7-4 and 7-5 illustrate that the drought indices clearly capture the high intensities of the droughts of 1983, 2000 and 2005 which devastated almost all parts of the country. In general, high magnitudes of annual rainfall totals translate into a smaller or negative index and vice-versa.

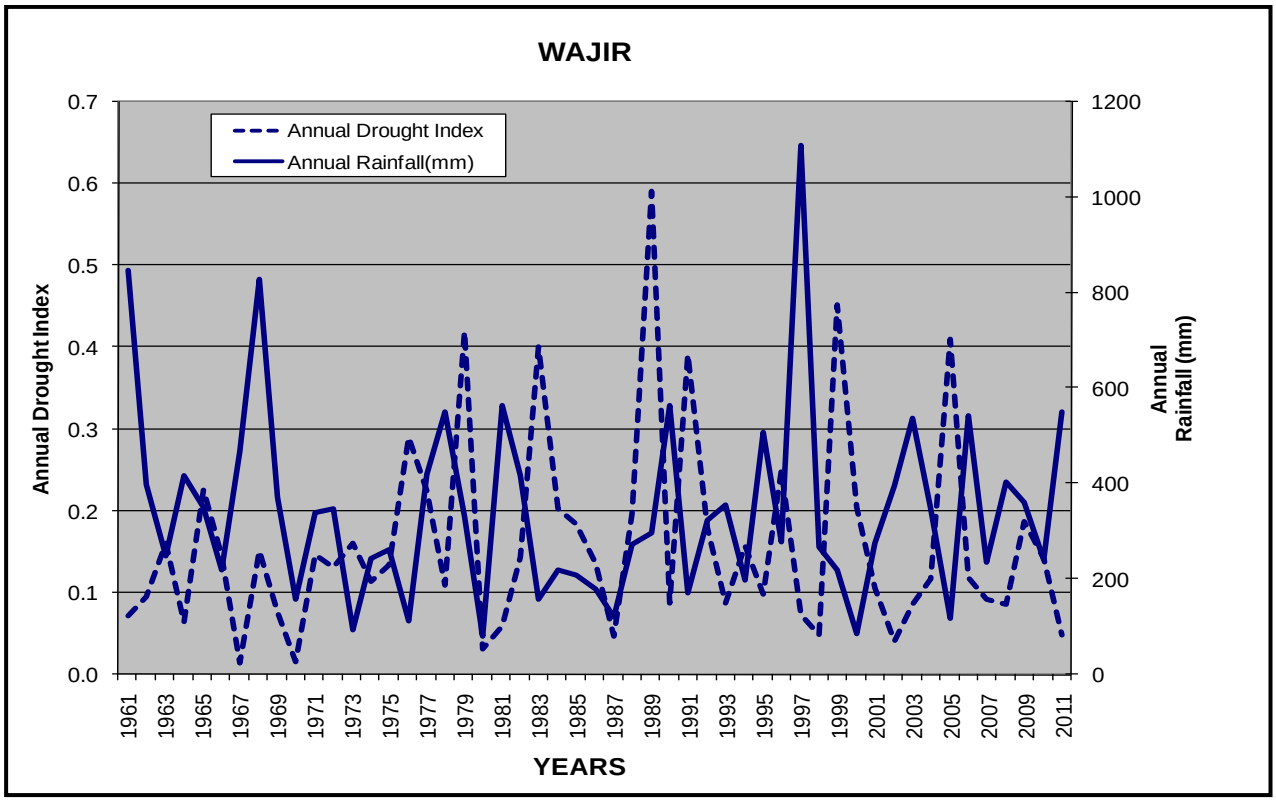

Figure 7-4 Distribution of the Annual Drought Index in Comparison to the Distribution of the Annual Rainfall in Wajir

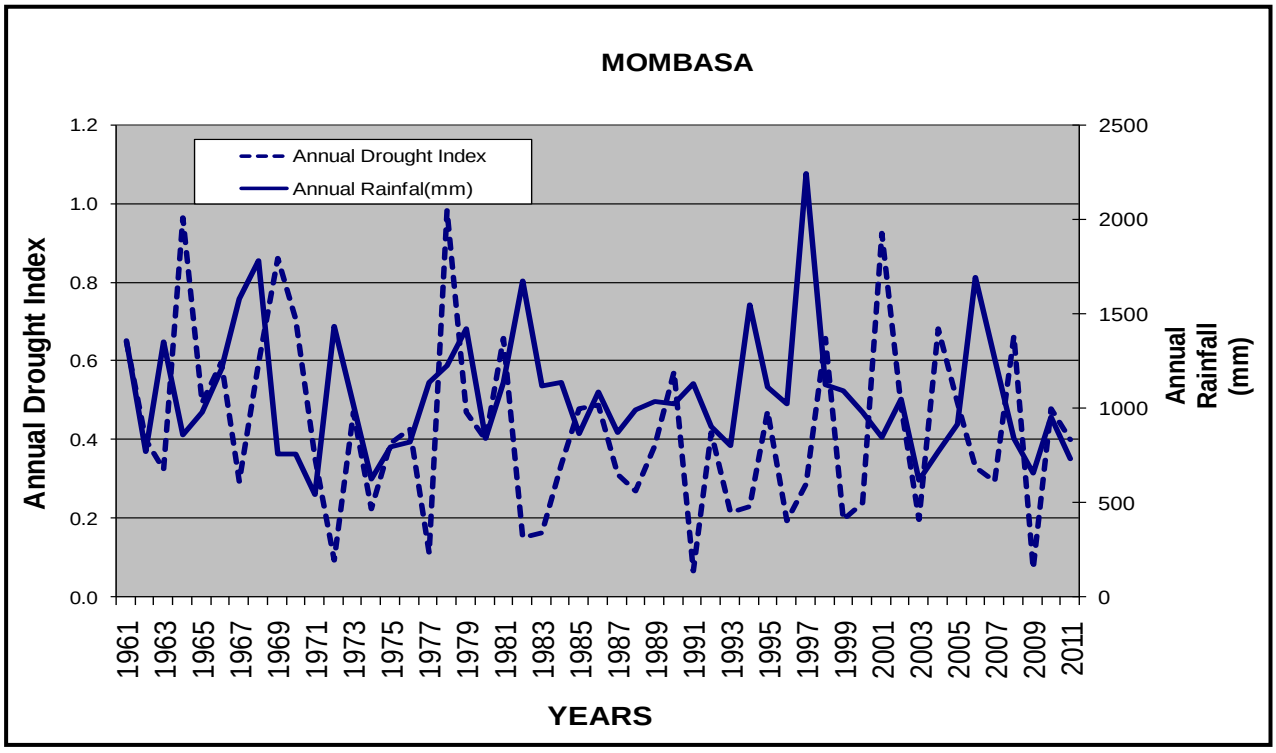

Figure 7-5 Distribution of the Annual Drought Index in Comparison to the Distribution of the Annual Rainfall in Mombasa.

The spatial distribution of mean annual drought indices in comparison to mean annual rainfall is shown in Figure 7-6 below. From the figure high mean annual values of the drought index are found in both areas of high and low mean annual rainfall. For example the western side of the country has drought index values of 0.5 yet it receives mean annual rainfall of above 1400mm, on the other hand the northeastern side which has mean annual rainfall of 400mm had drought index values above 0.5. The drought index therefore seems to differentiate dryness (having little or no rain throughout) from drought which can occur not only in the wet areas, but also in the dry areas of the country.

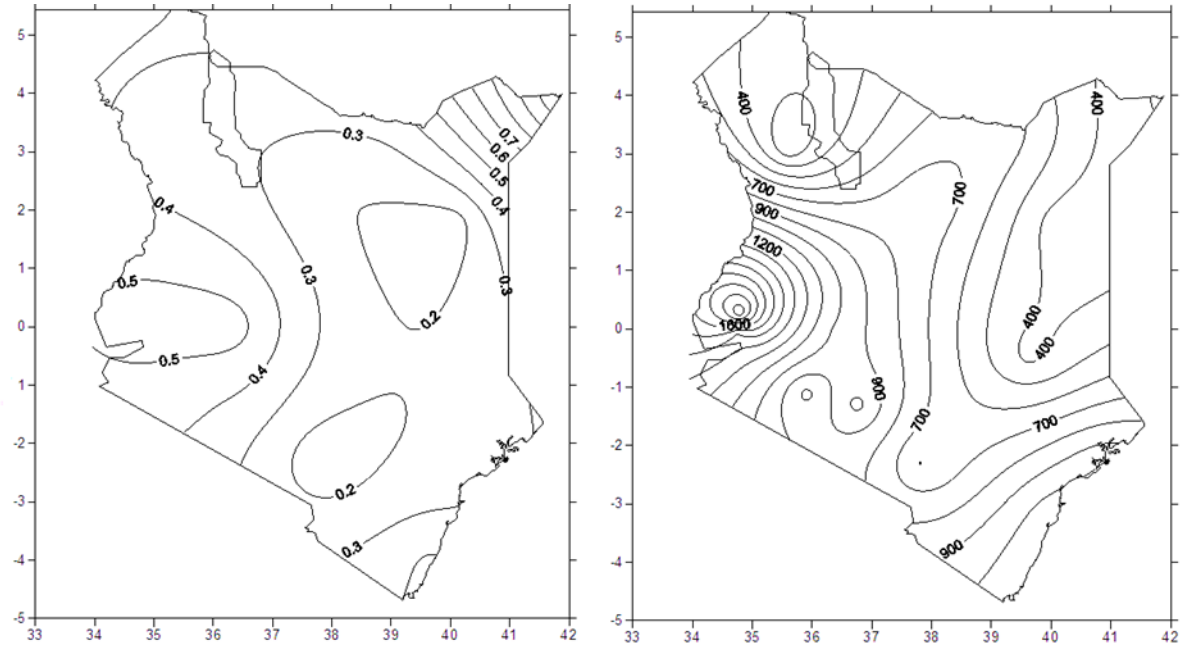

Figure 7-6 Spatial Distribution of mean Annual Drought Index (left panel) in comparison to mean Annual Rainfall (right panel) in Kenya.

The first step in this exercise was to define the most suitable probability distribution which was used. The following distributions which are often used were considered: Generalized Extreme Value, Generalized Pareto, Gumbel Max (Maximum Extreme Value Type I), and Gumbel Min (Minimum Extreme Value Type I). The distributions were calibrated by fitting them to the available data. Table 7-4 shows the estimated distribution parameters.

	Distribution	Parameters
1	Gen. Extreme Value	k=0.01006 σ=0.09382 μ=0.1547
2	Gen. Pareto	k=-0.40018 σ=0.22062 μ=0.05224
3	Gumbel Max	σ=0.09389 μ=0.15561
4	Gumbel Min	σ=0.09389 μ=0.264

Table 7-4 Distribution parameters

The distributions were further discriminated against each other using goodness of fit statistics. From the goodness of fit results given in Table 7-5 below, the General Extreme Value (GEV) distribution fits the best, because Kolmogorv-Smirnov and Anderson-Darling goodness of fit tests rank it at position 1. Hence the GEV distribution was adopted for further analysis .

	Distribution	Kolmogorov Smirnov		Anderson Darling		Chi-Squared	
		Statistic	Rank	Statistic	Rank	Statistic	Rank
1	Gen. Extreme Value	0.18674	1	2.0744	1	12.906	3
2	Gen. Pareto	0.1885	2	9.5146	4	N/A	
3	Gumbel Max	0.18896	3	2.0916	2	12.843	2
4	Gumbel Min	0.30891	4	5.2237	3	9.8067	1

Table 7-5 Goodness of fit

The General Extreme Value (GEV) distribution is a three-parameter distribution that combines the Gumbel, Frechet and Weibull maximum extreme value distributions. The three parameters are: k shape parameter, σ scale parameter and μ location parameter.

Its Probability Density Function (PDF) is given by:

$$f(x) = \begin{cases} \frac{1}{\sigma} \exp\left(-(1+k\,z)^{-1/k}\right)(1+k\,z)^{-1-1/k} & k \neq 0 \\ \frac{1}{\sigma} \exp(-z - \exp(-z)) & k = 0 \end{cases} \quad 7.4.3$$

Where $z \equiv \frac{x-\mu}{\sigma}$

The cumulative distribution function (CDF) of the distribution was used to calculate the annual exceedance probability (AEP), or the probability that an event is equaled or exceeded in any single year. To obtain the return period of the drought events, the reciprocal of the exceedance probability was calculated.

Results of the return period of the annual drought index magnitudes are shown in Table 7-6 and Figures 7-7 to 7-10. The results show that droughts with small magnitudes occur more frequently and have shorter return periods (of 1-2 years). This means that before communities in the country recover from a previous drought another one starts; this can be seen in the case of 2009 and 2010. These makes communities very vulnerable and deprives the little water resources that are harvested in the wet period in between the droughts. The occurrence of the drought frequently also hampers the governments development projects because resources are directed to the communities affected.

LODWAR		MARSABIT		DAGORETI		GARISSA		LAMU		KISUMU		LODWAR		NYAHURURU		MANDERA	
RP	ADI	T	ADI	T	ADI	T	ADI	T	ADI	T	ADI	T	ADI	T	ADI	T	ADI
1	0.2	1	0.1	1	0.1	1	0.1	1	0.1	1	0.4	1	0.2	1	0.4	1	0.2
2	0.3	2	0.2	2	0.2	2	0.2	2	0.2	2	0.5	2	0.3	2	0.5	2	0.5
5	0.4	5	0.3	5	0.3	5	0.3	5	0.7	5	0.7	5	0.4	5	0.6	4	1.3
14	0.5	14	0.4	14	0.4	14	0.4	14	0.5	14	0.8	14	0.6	14	0.9	14	3.1
25	0.7	25	0.5	25	0.5	25	0.5	25	0.6	25	0.9	25	0.7	25	1.0	25	3.9
100	1.0	100	0.8	100	0.7	100	0.6	100	0.7	100	1.2	100	1.0	100	1.2	100	5.5
	T - Return Period in years																
	ADI - Annual Drought Index																

Table 7-6 Return period of annual Drought Index over selected stations

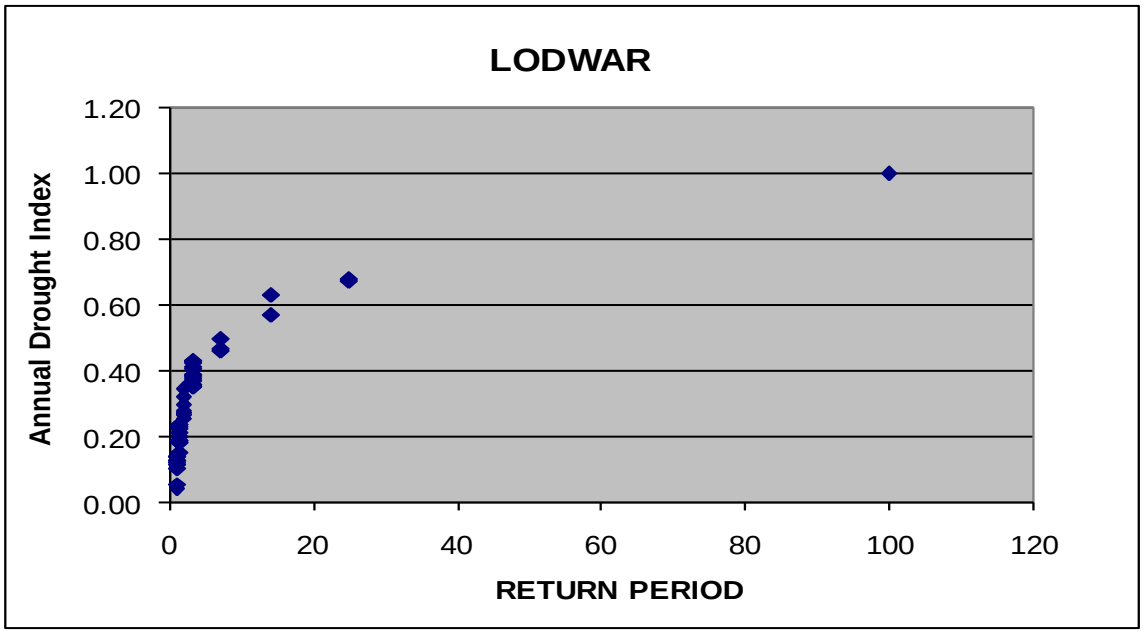

Figure 7-7 Return periods of drought magnitudes over Lodwar

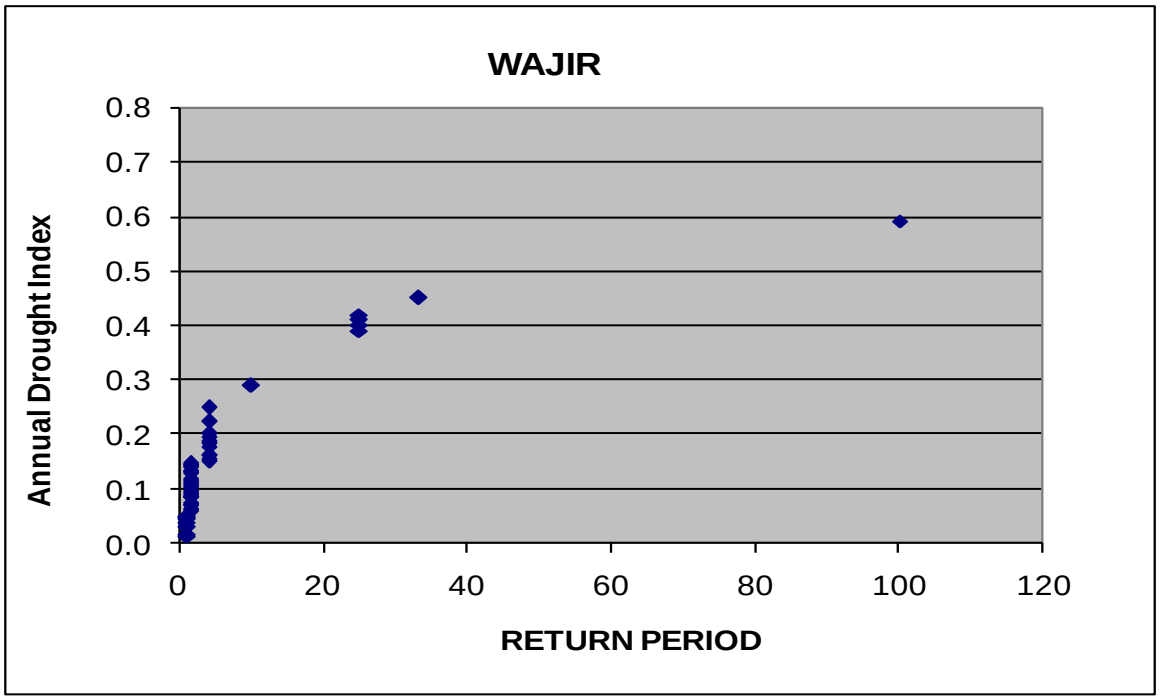

Figure 7-8 Return periods of drought magnitudes over Wajir

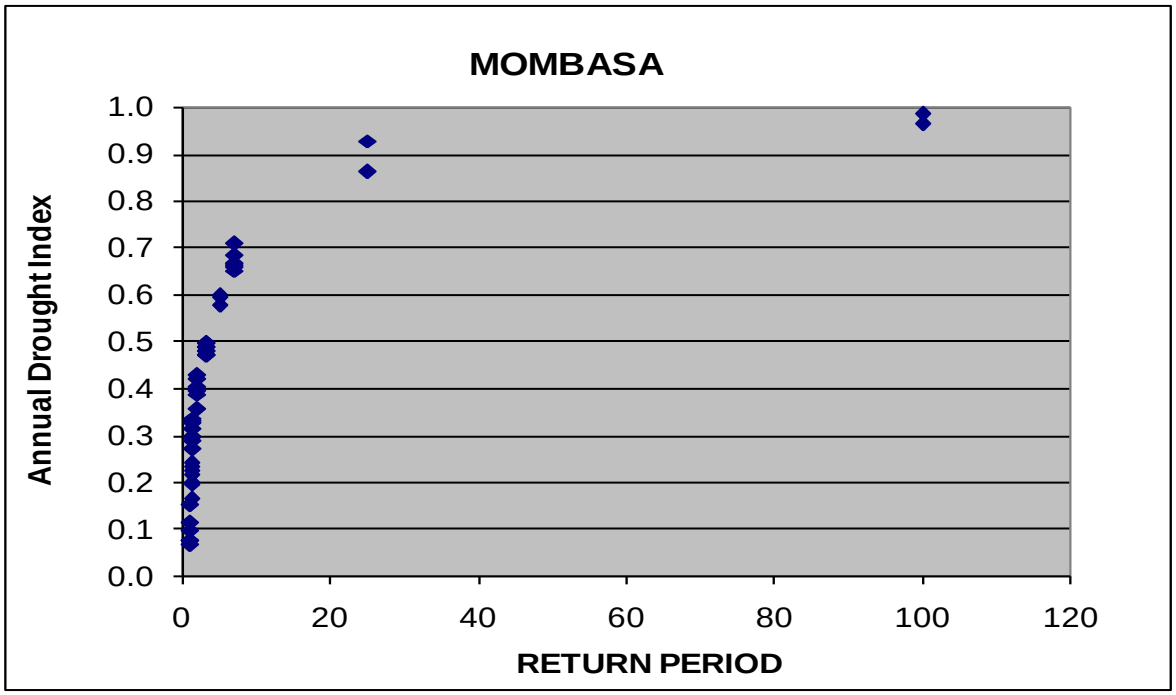

Figure 7-9 Return periods of drought magnitudes over Mombasa

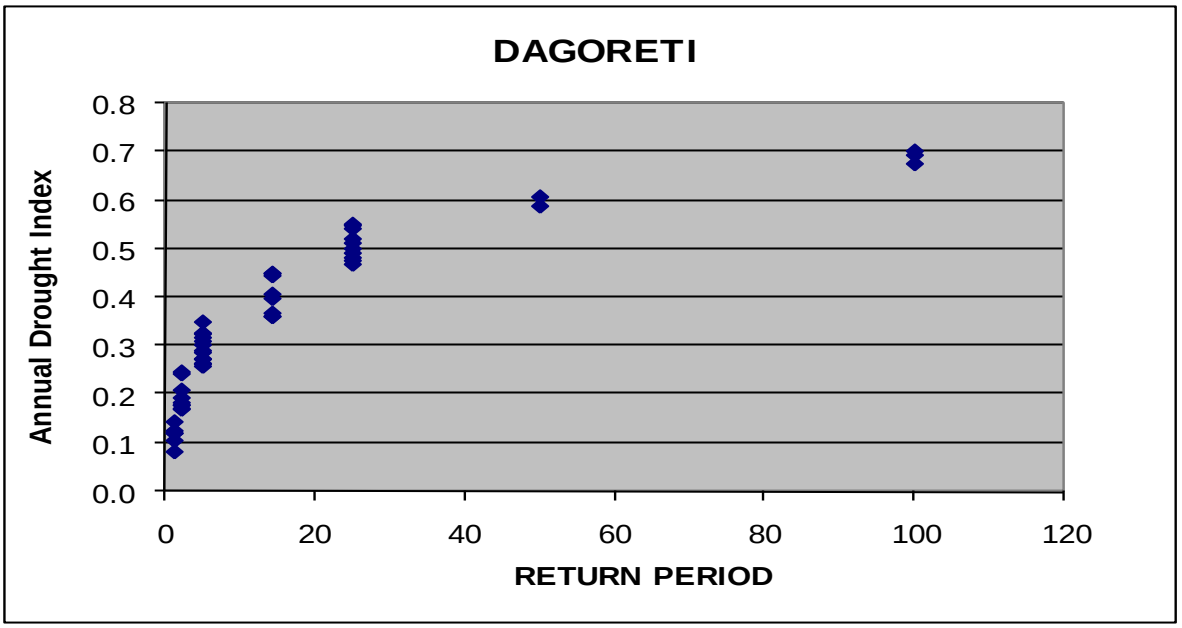

Figure 7-10 Return periods of drought magnitudes over Dagoreti

7.4.2 Drought Vulnerability

Vulnerability to drought has been known to be influenced by other factors besides rainfall deficit. Some of these factors include; population, poverty level and livelihood among others. High population could be indicative of high vulnerability, in terms of households' dependence on a decreasing supply of resources during drought events. Poverty level has a linear relationship with vulnerability.

Based on the above, the annual drought index results obtained in the previous section, poverty level data and population data were used to develop a drought risk map for Kenya as shown in Figures 7-11 and 7-12. The data was divided into terciles to determine thresholds, the various classes were combined to determine risk levels.

In Figure 7-11 are combined annual drought index and poverty level data. The results show that western region of the country, despite having moderate drought index, has medium vulnerability to drought because of the high poverty level. The sector that has high is based on high poverty levels but low annual drought index in some parts and in others medium poverty levels but high annual drought index. The sector with low vulnerability has low drought index and medium poverty levels in most areas. However, some parts like the Northwestern part of the country are classified as low vulnerability areas though from past drought events they have been found to be vulnerable; this disparity can be attributed to the scarce data over the area which has been extrapolated.

In Figure 7-12, we combine annual drought index and population data. The results indicate that based on the population and drought index the vulnerability levels are not high for most parts of the country and this could be attributed to the fact that population does not have a very direct correlation to drought vulnerability. For example the Northern part of the country is categorized under medium and low vulnerability because the population is low; however, when a drought event occurs nearly all the population in this area is affected.

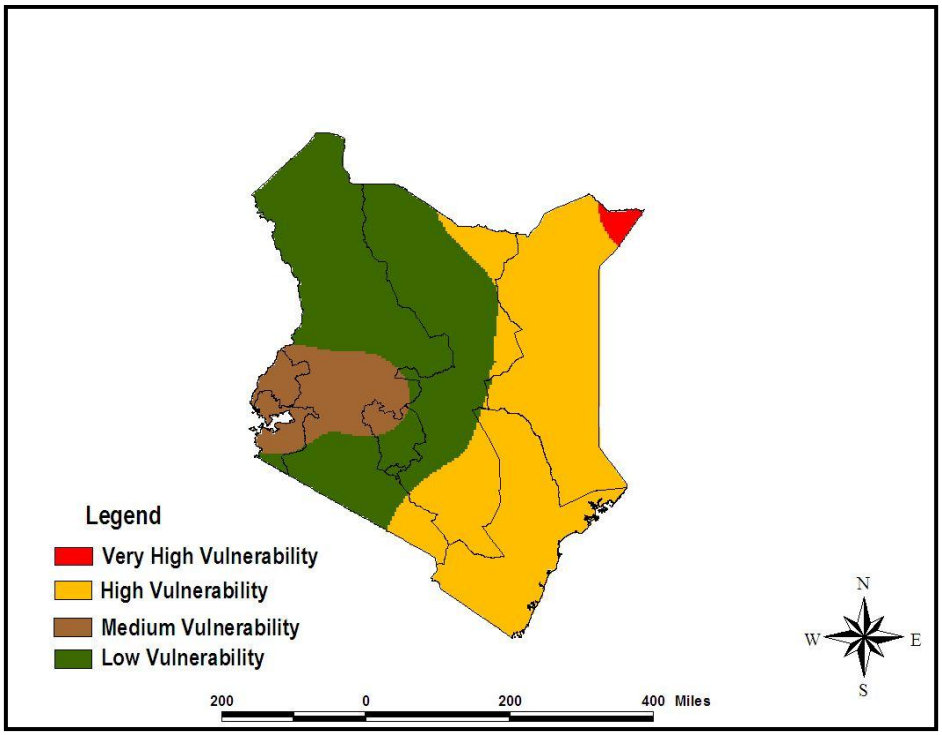

Figure 7-11 Kenya's Drought Risk map generated using annual drought index and poverty level

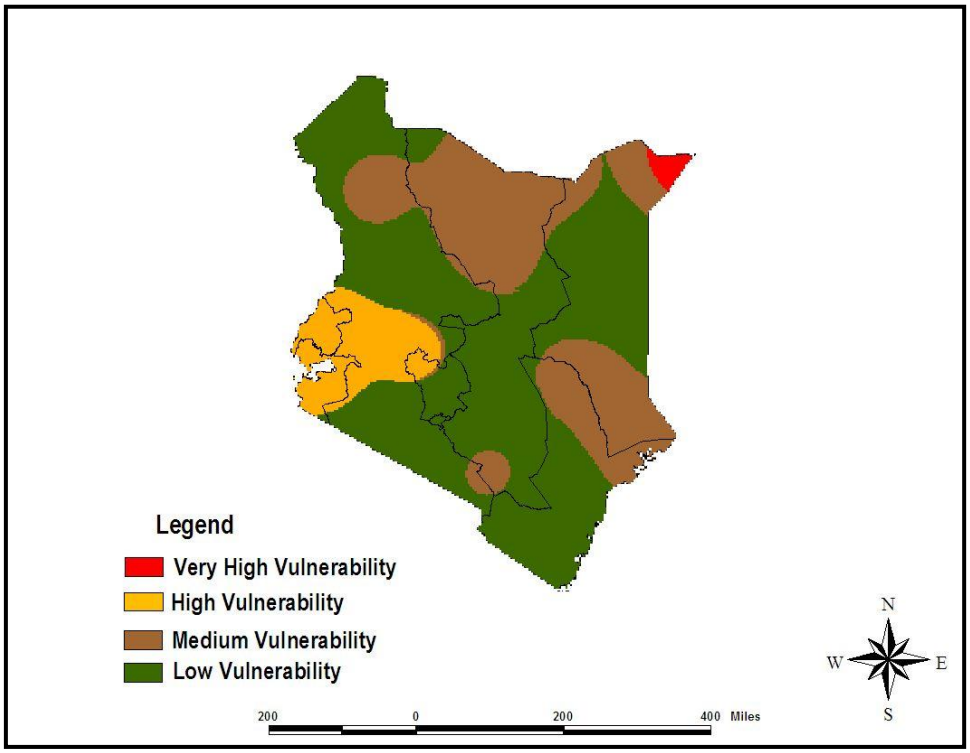

Figure 7-12 Kenya's Drought Risk map generated using annual drought index and population

It can be concluded that low magnitude drought events occur frequently over most parts of Kenya and these drought events have low return periods. The frequency of these events

makes the communities vulnerable to drought since there isn't enough time to recover from one drought. The major impact is reflected in food deficit and inadequate water supply for domestic, livestock watering and other uses.

Poverty levels are key in the vulnerability of communities to drought for example some areas that don't have high annual drought values are vulnerable because the communities there are poor and if a drought of a small magnitude occurs they are highly affected because they don't have buying power to be able to get resources from elsewhere.